1996

Experimental acoustic model for intake manifold testing.

Colin James. Novak
University of Windsor

National Library of Canada
Acquisitions and Bibliographic Services Branch
395 Wellington Street
Ottawa, Ontario
K1A 0N4

Bibliothèque nationale du Canada
Direction des acquisitions et des services bibliographiques
395, rue Wellington
Ottawa (Ontario)
K1A 0N4

Your file Votre référence

Our file Notre référence

NOTICE

The quality of this microform is heavily dependent upon the quality of the original thesis submitted for microfilming. Every effort has been made to ensure the highest quality of reproduction possible.

If pages are missing, contact the university which granted the degree.

Some pages may have indistinct print especially if the original pages were typed with a poor typewriter ribbon or if the university sent us an inferior photocopy.

AVIS

La qualité de cette microforme dépend grandement de la qualité de la thèse soumise au microfilmage. Nous avons tout fait pour assurer une qualité supérieure de reproduction.

S'il manque des pages, veuillez communiquer avec l'université qui a conféré le grade.

La qualité d'impression de certaines pages peut laisser à désirer, surtout si les pages originales ont été dactylographiées à l'aide d'un ruban usé ou si l'université nous a fait parvenir une photocopie de qualité inférieure.

Canada

EXPERIMENTAL ACOUSTIC MODEL FOR INTAKE MANIFOLD TESTING

by

Colin Novak

A Thesis
submitted to the
Faculty of Graduate Studies and Research
through the Department of
Mechanical Engineering in partial Fulfilment
of the requirements for the Degree of
Master of Applied Science
at the University of Windsor

Windsor, Ontario, Canada

1996

ISBN 0-612-11019-2

Name _____

Dissertation Abstracts International and *Masters Abstracts International* are arranged by broad, general subject categories. Please select the one subject which most nearly describes the content of your dissertation or thesis. Enter the corresponding four-digit code in the spaces provided.

AUTOMOTIVE

SUBJECT TERM

0540

SUBJECT CODE

UMI

Subject Categories

THE HUMANITIES AND SOCIAL SCIENCES

COMMUNICATIONS AND THE ARTS

Architecture 0729
Art History 0377
Cinema 0900
Dance 0378
Fine Arts 0357
Information Science 0723
Journalism 0391
Library Science 0399
Mass Communications 0708
Music 0413
Speech Communication 0459
Theater 0465

EDUCATION

General 0515
Administration 0514
Adult and Continuing 0516
Agricultural 0517
Art 0273
Bilingual and Multicultural 0282
Business 0688
Community College 0275
Curriculum and Instruction 0727
Early Childhood 0518
Elementary 0524
Finance 0277
Guidance and Counseling 0519
Health 0680
Higher 0745
History of 0520
Home Economics 0278
Industrial 0521
Language and Literature 0279
Mathematics 0280
Music 0522
Philosophy of 0998
Physical 0523
Psychology 0525
Reading 0535
Religious 0527
Sciences 0714
Secondary 0533
Social Sciences 0534
Sociology of 0340
Special 0529
Teacher Training 0530
Technology 0710
Tests and Measurements 0288
Vocational 0747

LANGUAGE, LITERATURE AND LINGUISTICS

Language
- General 0679
- Ancient 0289
- Linguistics 0290
- Modern 0291

Literature
- General 0401
- Classical 0294
- Comparative 0295
- Medieval 0297
- Modern 0298
- African 0316
- American 0591
- Asian 0305
- Canadian (English) 0352
- Canadian (French) 0355
- English 0593
- Germanic 0311
- Latin American 0312
- Middle Eastern 0315
- Romance 0313
- Slavic and East European 0314

PHILOSOPHY, RELIGION AND THEOLOGY

Philosophy 0422
Religion
- General 0318
- Biblical Studies 0321
- Clergy 0319
- History of 0320
- Philosophy of 0322

Theology 0469

SOCIAL SCIENCES

American Studies 0323
Anthropology
- Archaeology 0324
- Cultural 0326
- Physical 0327

Business Administration
- General 0310
- Accounting 0272
- Banking 0770
- Management 0454
- Marketing 0338

Canadian Studies 0385
Economics
- General 0501
- Agricultural 0503
- Commerce-Business 0505
- Finance 0508
- History 0509
- Labor 0510
- Theory 0511

Folklore 0358
Geography 0366
Gerontology 0351
History
- General 0578
- Ancient 0579
- Medieval 0581
- Modern 0582
- Black 0328
- African 0331
- Asia, Australia and Oceania 0332
- Canadian 0334
- European 0335
- Latin American 0336
- Middle Eastern 0333
- United States 0337

History of Science 0585
Law 0398
Political Science
- General 0615
- International Law and Relations 0616
- Public Administration 0617

Recreation 0814
Social Work 0452
Sociology
- General 0626
- Criminology and Penology 0627
- Demography 0938
- Ethnic and Racial Studies 0631
- Individual and Family Studies 0628
- Industrial and Labor Relations 0629
- Public and Social Welfare 0630
- Social Structure and Development 0700
- Theory and Methods 0344

Transportation 0709
Urban and Regional Planning 0999
Women's Studies 0453

THE SCIENCES AND ENGINEERING

BIOLOGICAL SCIENCES

Agriculture
- General 0473
- Agronomy 0285
- Animal Culture and Nutrition 0475
- Animal Pathology 0476
- Food Science and Technology 0359
- Forestry and Wildlife 0478
- Plant Culture 0479
- Plant Pathology 0480
- Plant Physiology 0817
- Range Management 0777
- Wood Technology 0746

Biology
- General 0306
- Anatomy 0287
- Biostatistics 0308
- Botany 0309
- Cell 0379
- Ecology 0329
- Entomology 0353
- Genetics 0369
- Limnology 0793
- Microbiology 0410
- Molecular 0307
- Neuroscience 0317
- Oceanography 0416
- Physiology 0433
- Radiation 0821
- Veterinary Science 0778
- Zoology 0472

Biophysics
- General 0786
- Medical 0760

EARTH SCIENCES

Biogeochemistry 0425
Geochemistry 0996
Geodesy 0370
Geology 0372
Geophysics 0373
Hydrology 0388
Mineralogy 0411
Paleobotany 0345
Paleoecology 0426
Paleontology 0418
Paleozoology 0985
Palynology 0427
Physical Geography 0368
Physical Oceanography 0415

HEALTH AND ENVIRONMENTAL SCIENCES

Environmental Sciences 0768
Health Sciences
- General 0566
- Audiology 0300
- Chemotherapy 0992
- Dentistry 0567
- Education 0350
- Hospital Management 0769
- Human Development 0758
- Immunology 0982
- Medicine and Surgery 0564
- Mental Health 0347
- Nursing 0569
- Nutrition 0570
- Obstetrics and Gynecology 0380
- Occupational Health and Therapy 0354
- Ophthalmology 0381
- Pathology 0571
- Pharmacology 0419
- Pharmacy 0572
- Physical Therapy 0382
- Public Health 0573
- Radiology 0574
- Recreation 0575
- Speech Pathology 0460
- Toxicology 0383

Home Economics 0386

PHYSICAL SCIENCES

Pure Sciences
Chemistry
- General 0485
- Agricultural 0749
- Analytical 0486
- Biochemistry 0487
- Inorganic 0488
- Nuclear 0738
- Organic 0490
- Pharmaceutical 0491
- Physical 0494
- Polymer 0495
- Radiation 0754

Mathematics 0405
Physics
- General 0605
- Acoustics 0986
- Astronomy and Astrophysics 0606
- Atmospheric Science 0608
- Atomic 0748
- Electronics and Electricity 0607
- Elementary Particles and High Energy 0798
- Fluid and Plasma 0759
- Molecular 0609
- Nuclear 0610
- Optics 0752
- Radiation 0756
- Solid State 0611

Statistics 0463

Applied Sciences
Applied Mechanics 0346
Computer Science 0984
Engineering
- General 0537
- Aerospace 0538
- Agricultural 0539
- Automotive 0540
- Biomedical 0541
- Chemical 0542
- Civil 0543
- Electronics and Electrical 0544
- Heat and Thermodynamics 0348
- Hydraulic 0545
- Industrial 0546
- Marine 0547
- Materials Science 0794
- Mechanical 0548
- Metallurgy 0743
- Mining 0551
- Nuclear 0552
- Packaging 0549
- Petroleum 0765
- Sanitary and Municipal 0554
- System Science 0790

Geotechnology 0428
Operations Research 0796
Plastics Technology 0795
Textile Technology 0994

PSYCHOLOGY

General 0621
Behavioral 0384
Clinical 0622
Developmental 0620
Experimental 0623
Industrial 0624
Personality 0625
Physiological 0989
Psychobiology 0349
Psychometrics 0632
Social 0451

ABSTRACT

This study was undertaken to see if the pressure pulses which propagate through an automobile induction manifold could be simulated using a computer generated signal fed into amplified speakers attached to a bench mounted intake manifold. To verify the legitimacy of the simulated pressure pulses, the noise emitted from the throttle body was measured and compared to the results of the theoretical Ricardo Wave Model and to similar measurements performed on a operating engine.

The pressure signal was generated using a computer program created with National Instruments' LabView software and a digital to analogue acquisition card mounted in a personal computer. The input data to this program was taken from the Ricardo Wave Model at an engine RPM of 2400. The noise measured at the throttle body was digitized using a second acquisition card and analyzed by another program, also created with LabView. The analysis program determined the time and frequency domain content of the measured signal for both the simulation model and the actual engine.

It was found that the two measured time domain signals compared favourably to the predicted theoretical time domain curve. The small differences in the experimentally generated time domain signal were accounted to non-linearities in the performance of the speakers used to generate the pressure pulses. The calculated mean and standard deviations for the two measured time signals also compared favourably which was further

reinforced by the determination of the correlation coefficient and covariance of the two signals.

The Fast Fourier Transform (FFT) analysis provided analogous results between the predicted theoretical and two measured signals with a fundamental frequency at approximately 80 Hz and second and third harmonics occurring at 160 Hz and 240 Hz respectively.

While the pressure pulses produced by the experimental simulation model at 2400 RPM closely paralleled the results produced by the theoretical model and actual engine, it is recommended that additional tests be performed at different RPMs. This would, however, require speakers better capable of producing lower frequencies and a faster computer in order to simultaneously generate the pressure signal and perform all analysis in real time.

Dedicated to
Alecia and furry family members

ACKNOWLEDGEMENTS

Sincere gratitude is extended to my supervisor and friend, Dr. R. G. Gaspar, for his kindness, guidance and efforts for ensuring that this research project was possible. Thanks is also extended to my committee members, Dr. Z. Reif and Dr. R. Du for all their assistance

Special recognition is given to Mr. P. Daly of Siemens Automotive for providing both the opportunity and financial assistance necessary to have made this project feasible.

Most importantly, my warmest acknowledgements are directed to Alecia and other family members and friends who persevered and provided encouragement throughout the period of this study.

TABLE OF CONTENTS

LIST OF FIGURES

LIST OF TABLES

Page

NOMENCLATURE

A/D	analogue to digital
BDC	bottom dead centre
DAT	digital audio tape
dB	decibels
D/A	digital to analogue
DC	direct current
DFT	discrete fourier transform
FEM	finite element modelling
FFT	fast fourier transform
Hz	hertz (cycles per second)
P_{ref}	reference pressure
P_{sys}	system pressure
RMS	root mean square
RPM	revolutions per minute
TDA	time domain averaging
TDC	top dead centre
V_{ref}	reference voltage
V_{sys}	system voltage

μ	mean
ρ	correlation coefficient
σ	standard deviation

I. INTRODUCTION

There are a large number of moving parts and associated processes involved with the operation of a modern day internal combustion powered vehicle. Given such conditions, one should not be surprised at the amount of noise that can be heard within the passenger compartment of the vehicle. Some of the causes of this noise include the combustion process of the engine, exterior wind noise, particularly at high speeds, tire noise as well as exhaust and intake noise. Many improvements have been made in recent years with stiffer and better acoustically insulated car bodies, more aerodynamic body designs, better tire technology and quieter muffler systems. While these efforts have improved the overall sound levels within the passenger compartment, it has made some of the other potential noise sources, induction noise in particular, more noticeable. This has resulted in greater efforts being taken in the study of induction noise and what may be done to lessen its impact on the overall comfort of the consumer.

The advent of smaller vehicles with less space under the hood coupled with the increased number of engine components, largely due to emissions controls, impose significant limitations on design engineers in the area of noise control. As a result, it is not always possible to design an induction manifold to be as quiet as possible while maintaining minimum flow requirement objectives as well as space and weight allocation under the hood. In answer to this, engineers may chose to 'tune' the manifold as opposed to reducing its overall sound level. All sound levels can be measured

empirically by engineers. Customers, however, may be more concerned with the quality, and not the quantity of sound, within reason. Therefore, if the attenuation efforts have been maximized to their potential, efforts can then be made to the production of a more pleasing sound [14]. This is illustrated by the positive influence on the car buyer by the solid thud of a car door or the muscular purr of a sports car at idle.

In order to achieve the above, efforts must be made in developing new research and design methods for induction systems. This begins with an understanding of what causes inlet noise.

Inlet noise is caused by a number of mechanisms. These mechanisms include the influence on the intake air by the operation of the intake valves, the physical parameters of the manifold ducting and any other attached accessories. Inlet noise is the audible result of the oscillation of intake air at the natural frequency of the inlet passage column. This oscillation is caused by a sharp pulse when the intake valve opens to the cylinder which has a pressure greater than atmospheric, thus resulting in a pulse. At the same time, a high frequency noise is generated at approximately 1000 Hz by the intake air travelling across the valve seat at a high velocity. These noise impulses, however, are usually reduced significantly to 80 - 150 Hz in the engine firing range due to the influence of the manifold ducting, silencers and air cleaner. A second oscillation occurs when the intake valve closes [13]. These two oscillations are illustrated in Figure 1.1.

The objective of this thesis was to develop an experimental model that would simulate the pressure pulses which propagate through a production intake manifold under

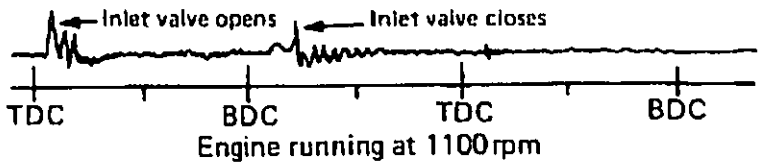

Figure 1.1: Inlet Noise Oscillogram [13]

operating conditions. Further, the experimental model had to be flexible enough in design so it could be easily adapted to any particular intake manifold. To achieve this, all physical parameters imposed on the experimental model are controlled by a personal computer taking any information specific to a given manifold from a spreadsheet data file. The intent of this thesis was not to eliminate the causes of intake noise or to conceptionalize a new manifold design capable of massive attenuation while maintaining required flow conditions.

The primary reason for developing this benchtop device and simulator model was to develop a tool which would facilitate future research in areas that are currently difficult or impossible to achieve with other experimental or numerical techniques. Examples of such research would be the effects of fuel wall wetting within the manifold or perhaps the potential interactions caused by these pressure pulses and the future use of different alternative fuels.

In order to simulate the pressure pulses, a known quantity of manifold data was required to mimic as input data into the experiment. The manifold data is also required to compare the results, or output information from the experimental model. The Ricardo Wave Model, a theoretical computer model used by Siemens Automotive, was chosen to serve this purpose. The Ricardo program provided pressure data for the manifold runners which was to be simulated in the experiment. The Ricardo program also provided predicted pressure data at the throttle body which could be compared to the measured data produced by the experimental model. Additionally, measurements at the throttle body of an operating engine were made and compared to the results produced by the experimental model to further reinforce the validity of this modelling technique.

II. LITERATURE SURVEY

The stated focus of this thesis is to simulate the pressure pulses in an intake manifold caused by the valve action of the engine through the use of analog data generated by a computer. The following literature survey was conducted to determine if any such or similar work has already been done by others. A thorough search was unable to reveal any literature which indicates that this specific project has been carried out in the past. However, it is apparent from the review of related literature that much research has been done in the study of induction noise. A review of these studies is essential to accumulate both an understanding of the fundamental analysis tools available as well as to gain a better comprehension of what can be achieved from continuing this type of research.

The manner in which intake manifold noise has been studied can be broken down into two primary categories, being Experimental Testing and Theoretical or Numerical Modelling. Experimental testing usually involves the testing of either a complete engine and manifold setup with actual operating conditions or a bench test with simulated operating conditions. Theoretical modelling involves either the implementation of generally accepted mathematical representations with simplifying assumptions and the use of computer programs or the application of finite element modelling (FEM).

The above primary categories can be further reduced down to two subcategories, being Internal and Surface Effects. Internal effects involve the study of the acoustical and fluidic characteristics inside the structure of the manifold and what can be done to

manipulate these in order to achieve a desired outcome. The study of the surface effects of the intake manifold involve the characterization of both acoustical and vibratory energy and how these vary given different manifold design conditions. These topics will be covered in the following sections in order to familiarize the reader with the different approaches taken to date.

2.1 Experimental Testing

Many believe that the experimental approach to manifold testing is the most efficient means to determine the actual characteristics of a system. Schellino [21] stated that he preferred experimental testing of intake manifolds over any numerical methods available. While this may be so in some circumstances, there is just as strong an argument on the numerical methods side that will be explored in a later section.

As already mentioned, experimental testing of intake manifolds may be done on either an operating engine or on a simulating test bench. The method to be used is largely dependant on the measured variables. If for instance, it is important to maintain the volumetric efficiency in the manifold while evaluating acoustical performance, the experiment would most likely be executed on an operating engine. However, if it were critical that all other acoustical influences be eliminated, testing would most likely be done under the controlled conditions of a bench test often in an anechoic chamber.

Much experimental work has concentrated on either the internal acoustical effects of the intake manifold or the exterior or surface effects. Internal effects deal with optimizing the acoustical design of the manifold, often through the implementation of a

Helmholtz resonator. Surface noise studies, which also include the area of vibrations, focus on the stiffness of the manifold structure and how this can be optimized. Each of these areas are explored in greater detail below.

2.1.1 Internal Effects

Through the opening and closing action of the intake valves in an engine head, pressure pulses are produced which propagate through the intake manifold. As a result of these pressure pulses, or air column oscillations, intake noise is created. This intake noise may be amplified by air column resonance or it may be dampened through the influence of the air cleaner [14]. As a result, both the magnitude and characteristics of intake noise can vary significantly from one engine model to another. The goal in studying these internal interactions in the intake manifold are to better understand how different design criteria influence the air column resonances or intake noise.

Jon W. Parsons [16] and K.S. Peat et al. [18] used an experimental test bench to investigate a 400 Hz boom in the induction system of a Jaguar V12 engine operating at 4000 RPM. The schematic layout of the test is illustrate in Figure 2.1. The noise source used to excite the system was an electromagnetic sound source of high acoustic impedance similar to a conventional pressure unit used to drive horn loudspeakers. A microphone located at the output of the manifold picked up the resulting noise and sent this information to the analyzer. Separate measurements were made for both the test system and a known reference system thus allowing determination of an overall insertion loss between the two systems. This was first done by determining the transfer function

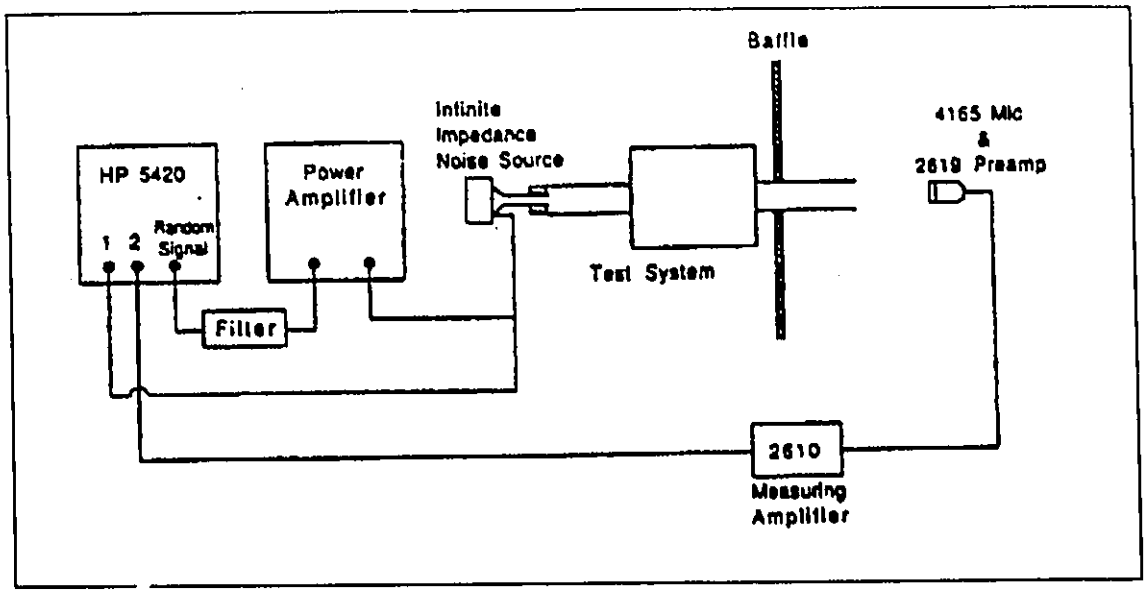

Figure 2.1: Schematic of Test Equipment used by Peat [16]

between the microphone noise and the voltage at the noise source for both the test and reference systems. The insertion loss was then calculated by the division of the two transfer functions as represented by the equation below, where P is the sound pressure level at the microphone and V is the sound source input voltage.

$$\text{Insertion Loss} = (P_{ref}/V_{ref})*(V_{sys}/P_{sys}) \qquad (2.1)$$

Once analyzed, it became apparent that the problems at 400 Hz were due to the length and volume of the ductwork and air cleaner box respectively. However, since

these parameters were fixed, a remedy was found by installing tuning holes in the inlet venturi. The effectiveness of the solution was reinforced by repeating the experiment.

Schellino et al. [21] set up an experimental setup to verify the results of a numerical FEM analysis used to determine the acoustic modes of the fluid inside the manifold. The experimental setup included a loudspeaker and reference microphone located at the manifold entrance as well as a number of measuring microphones used to measure the internal sound pressure along the centreline of the manifold duct. The loudspeaker produced a sine-sweep signal in the 300 - 500 Hz frequency range. The resultant acoustic measurements were in the form of transfer functions between the pressure levels measured by the internal microphones and that of the exciter measured by the reference microphone. It was determined that the measurements had close correlation to the numerical results.

Payri et al. [17] employed the three microphone method which allowed calculation of the frequency spectrum at the inlet and outlet of the manifold. The excitation source was described only as a pulsating flow test rig used to generate pressure wave amplitudes and mean flow in the same order of magnitude as the actual engine. The goal once again was to verify results of an analytical model to experimental results.

Nishio et al. [14] of Japan was concerned that the study of induction noise was usually an afterthought in the design stages of the intake manifold, with volumetric efficiency always given the priority. To eliminate this, Nishio developed a test system called the Pulsation Simulator which would facilitate the study of air intake noise reduction at an early stage and in parallel with the study of volumetric efficiency.

The system as illustrated in Figure 2.2 reproduced intake pulsations and flow precisely in the actual engine using its cylinder head.

The pressure pulses were created by the action of the intake valves which was operated by a variable speed electric motor. Negative pressure, to reproduce the air intake inertia effects, is created by a vacuum pump at the exhaust manifold. Air flow rates for the system were controlled and measured by critical flow, or sonic nozzles. Noise measurements were made with a microphone located at the inlet of the air intake system.

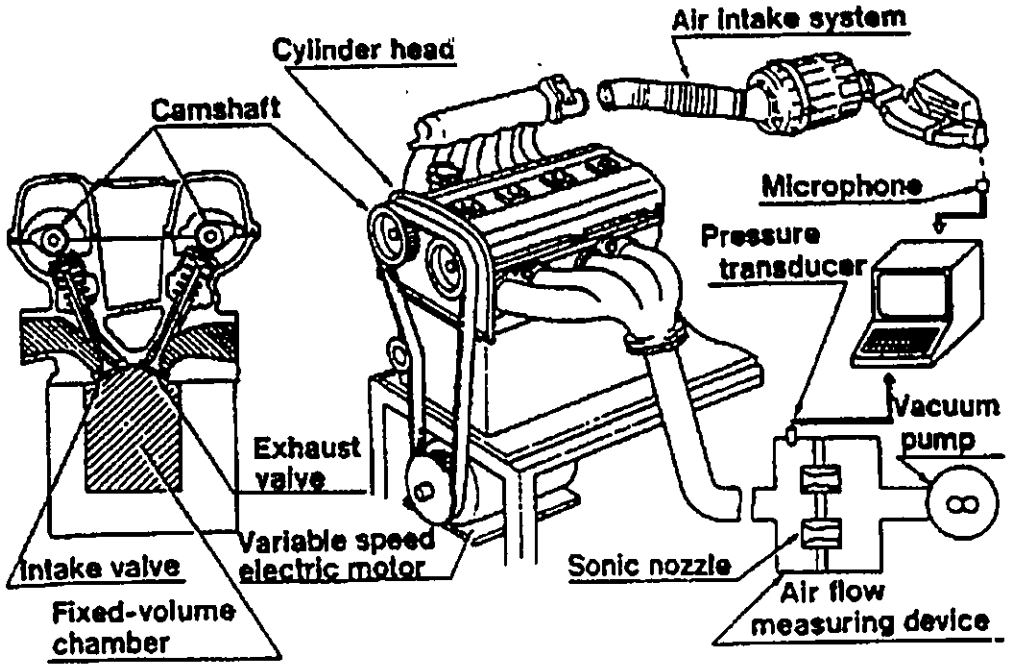

Figure 2.2: Pulsation Simulator [14]

When compared to measurements of an actual engine, it was shown that both volumetric efficiency and sound pressure levels produced by the Pulsation Simulator had good correlation as illustrated in Figures 2.3 and 2.4.

Using this simulator, Nishio [14] demonstrated that optimization of resonator design, usually conducted at the final stages of engine development, can be conducted at an earlier stage in parallel to volumetric efficiency tests.

2.1.2 **Surface Effects**

The need to study noise emissions from the surface or shell of the intake manifold is the manifestation of thinner and or alternative materials being employed in the manufacturing of automotive parts. While lighter gauge metals and plastic materials are cheaper in material and manufacturing costs and more importantly result in a lower overall weight of the vehicle, they may impose acoustical problems associated with their lower density. The general solution in the past was to replace the part with another of higher density so as to control transmission loss. This however, results in the reduction of design flexibility, possible part integrity and potential weight and cost advantages [5].

W. W. Kraft et al. [5] of BASF used noise intensity measurements in addition to experimental modal analysis and holographic analysis to compare the noise emissions from both a plastic and an aluminum manifold. The aluminum manifold had twice the thickness of the plastic one which meant it was also much heavier. The tests were repeated with a modified plastic manifold which had been stiffened with the addition of

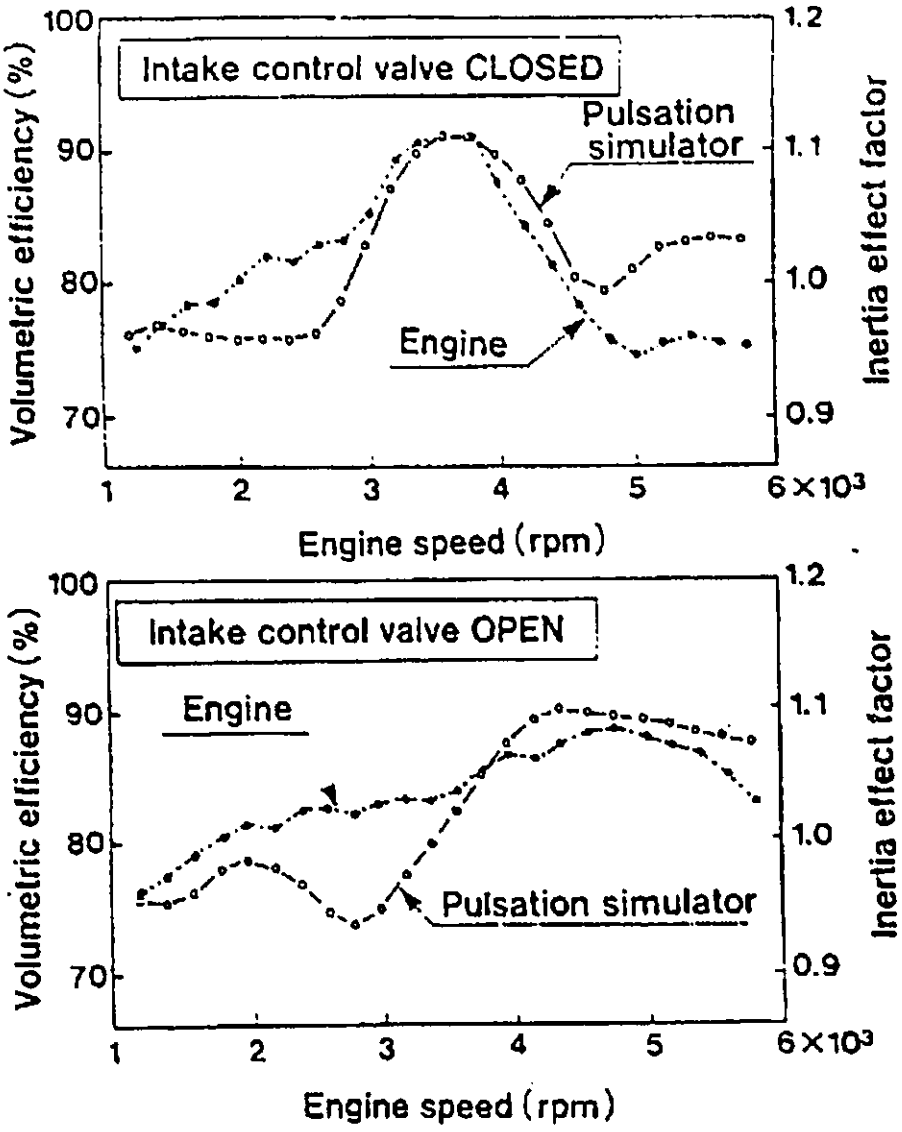

Figure 2.3: Volumetric Efficiency Obtained from the Pulsation Simulator and the Actual Engine [14]

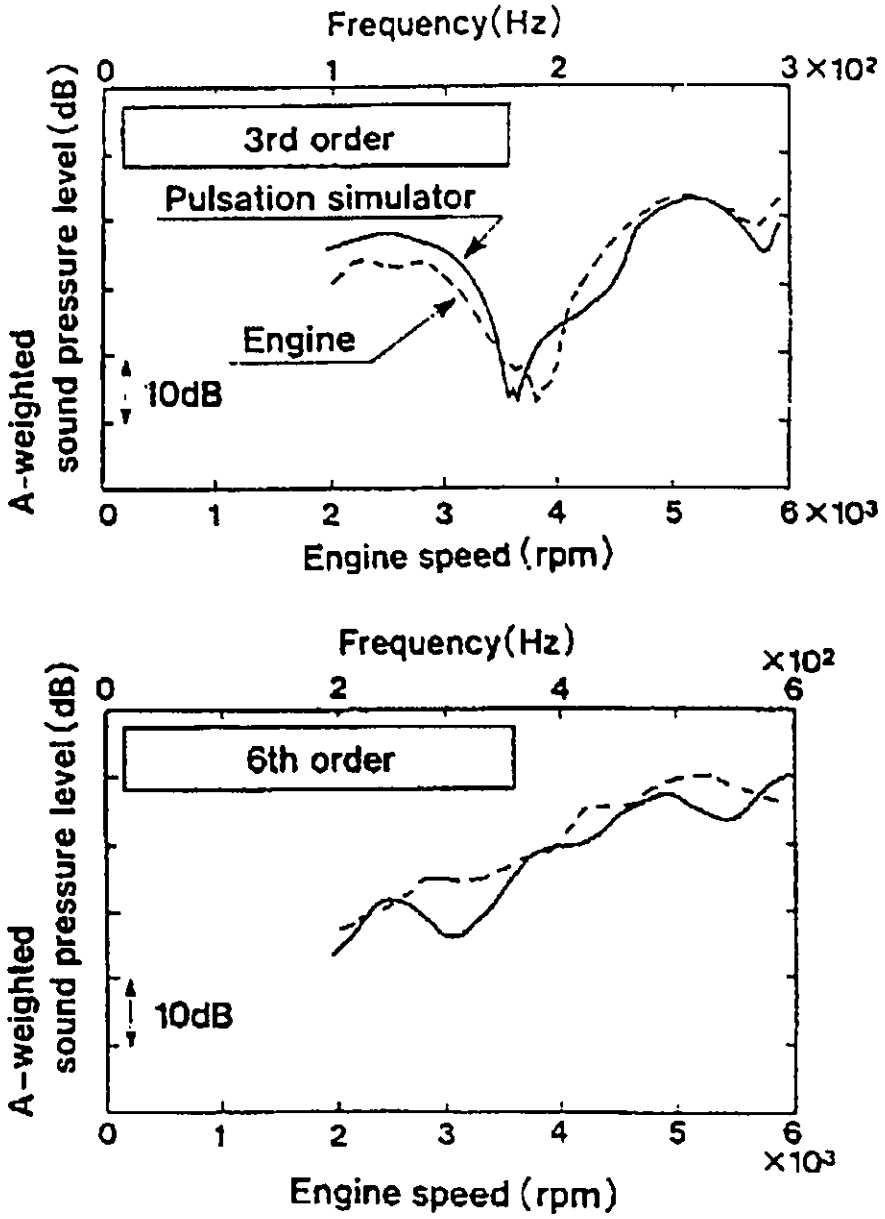

Figure 2.4: Intake Noise Characteristics Obtained from the Pulsation Simulator and the Actual Engine [14]

ribs and modifications to wall thickness at specific locations. Through this iterative optimization process, the resulting plastic manifold had a significant reduction in thickness. A flow chart illustrating the process taken by Kraft [5] is reproduced in Figure 2.5. The tests were then repeated by measuring vibration as shown in Figure 2.6. It was also shown that the overall noise levels emitted from the modified manifold compared closely to the much heavier aluminum manifold as illustrated in Figure 2.7.

2.2 Theoretical Modelling

In most cases, experimental testing will provide results as close to actual conditions as possible. This is due to the elimination of many simplifying assumptions related to both the physical characteristics and internal flow conditions used in analytical methods. In some cases, however, theoretical modelling has proven to be a useful tool for manifold design. The fundamental obstacle to overcome in theoretical modelling is to ensure that any influences from the engine and other individual elements in the system are understood and accounted for. On the other hand, "the primary benefit is seen to be in the reduction of development cycle times and cost of prototype systems" [16].

2.2.1 Internal Effects

Parsons [16] and Peat [18] used a modelling software package, LAMPS, developed in part by Loughborough University, to determine the insertion loss in induction manifolds. Using an input data file containing the geometry, temperature and gas flow

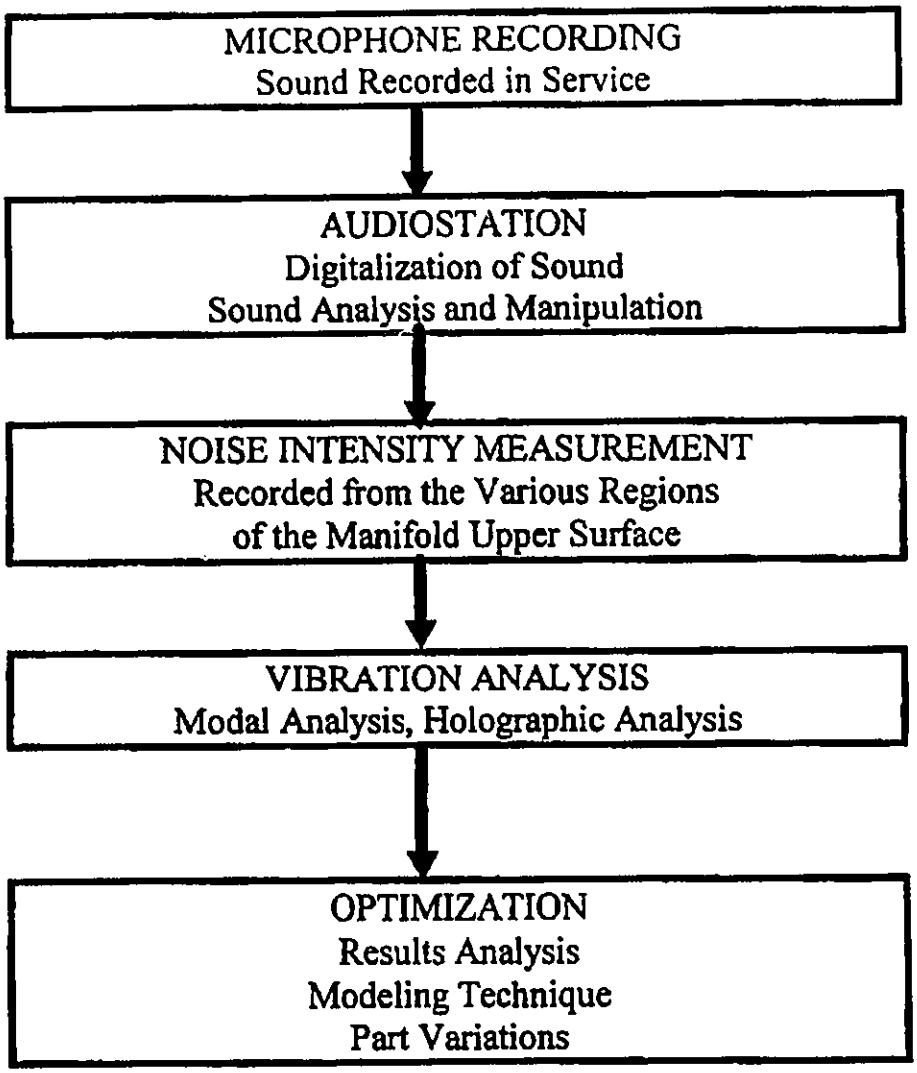

Figure 2.5: Flow Chart Illustrating Optimization Process [5]

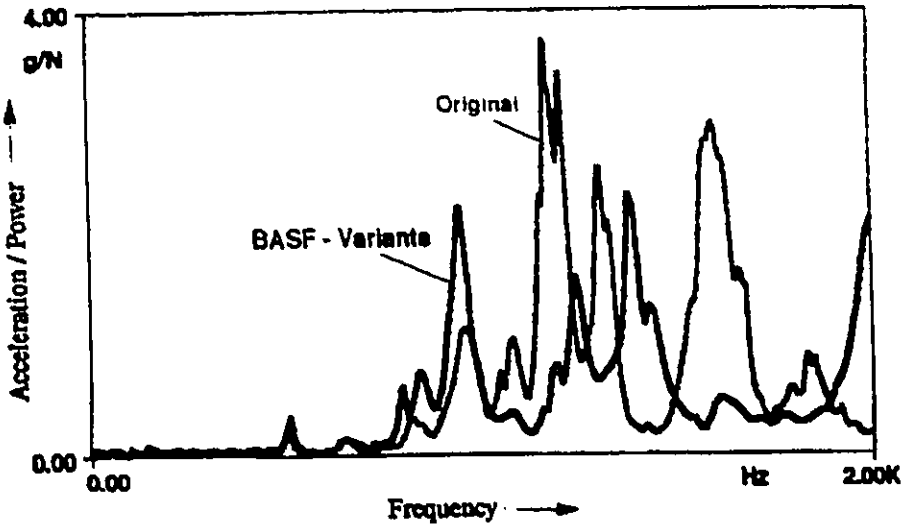

Figure 2.6: Transform Function of Original and Optimized Manifolds [5]

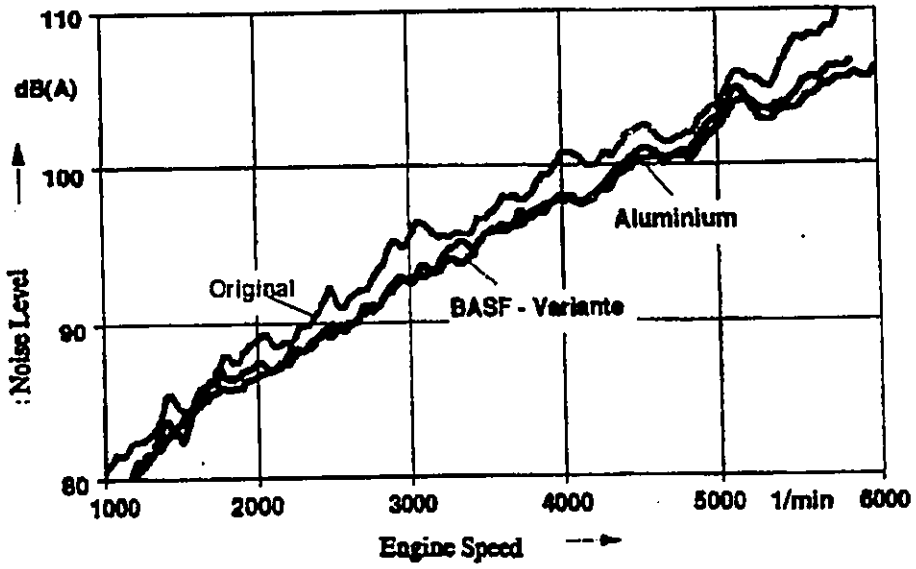

Figure 2.7: Overall Noise Recorded from an Aluminum, an Un-Optimized, and an Optimized Manifold [5]

characteristics of the system under consideration, the software package utilizes a transfer matrix approach assuming a linear one dimensional theory to model the acoustics through the manifold. It was proven that within the frequency range of concern, the computer model provided good correlation with the experimental results as described in section 2.1.2 of this thesis. This is shown in Figure 2.8 which illustrates the theoretical and experimental results of a Jaguar V12 manifold along with identifiers of any significant variations.

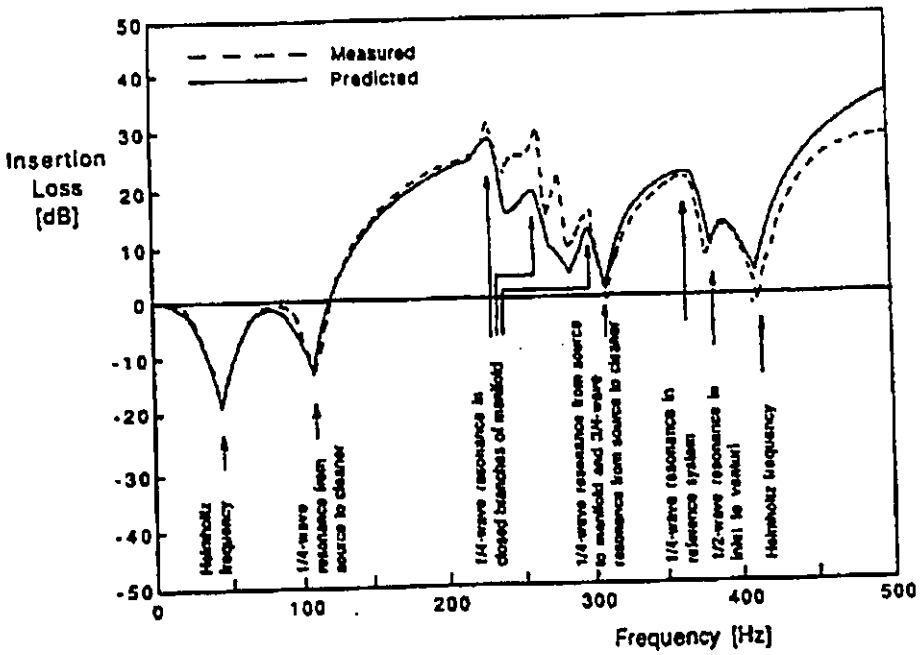

Figure 2.8: Measure and Predicted Insertion Loss [16]

Schellino [21] employed two numerical models, both built within the Sysnoise software package. The first one described later on in section 2.2.2 employs a surface analysis. The second model, using FEM, "was used to determine the acoustic modes of the fluid located inside the intake duct" [21]. The model contained a volumetric mesh to represent the air volume in the duct where the walls were assumed rigid. The duct wall was represented by a zero velocity boundary condition. The open ends of the duct were modelled with a zero pressure boundary condition. Using this approach, the first 20 acoustic modes were determined and were found to be similar to those found in experimental tests as described in section 2.1.1.

2.2.2 **Surface Effects**

Surface noise, which as implied earlier, is largely dependant on structure stiffness, may also be modelled by numerical methods. The most popular of these would be finite element analysis.

Schellino [21] was able to predict the coupled structural-acoustic frequency response of a manifold using a finite element/acoustic boundary element method. This model employed a surface mesh to represent the shell of the manifold which allowed the calculation of the frequency response function for the manifold. When compared to experimental results, the numerical simulation was very close with the presence of some differences being explained by the fact that no structural damping was included in the numerical calculations.

III. EXPERIMENTAL DETAILS

As in any experiment, it is important that the data collected be meaningful, repeatable and in conformance to any physical and theoretical restrictions imposed by the measurement systems. In order to ensure this, an understanding of the experimental procedure and equipment used is paramount. The following sections will describe the equipment and instrumentation selected, the design and preparation of the experiment and a description of the tests done on the system.

3.1 Equipment and Instrumentation

The equipment and instrumentation used to facilitate the experimental procedure can be classified into four separate areas being:

1. Equipment and instrumentation used to generate the synthesized waveform.
2. Experimental air intake manifold model and associated equipment and instrumentation used to simulate operating conditions.
3. Equipment and instrumentation used for acquiring and analyzing the modelled data.
4. Equipment and instrumentation used to acquire induction noise from the operating Neon engine.

3.1.1 Equipment used to Generate Waveform

The primary focus of the experiment is to simulate the pressure pulses within the intake manifold with some sort of pressure induction devise. However, irrespective of

what this device may be, focus must first be on the generation of a signal to excite such a device. A National Instruments AT-AO-10 high performance 12-bit ten channel digital to analog output board was chosen to serve this purpose. This board was housed in a 486 DX4-100 computer. Although only four channels were necessary to fulfil the experimental requirements on the manifold under study, it was desired to have the capability to output to a minimum of eight channels to accommodate the potential testing of different manifolds. A more thorough description of the technical characteristics of the analog output board can be found in Appendix A and in the references [10][11][12].

A computer program was created to control the D/A board using National Instruments' LabView software package. This graphical based programming package was used to synthesize communications between the user, a Quattro spreadsheet containing the raw waveform data and the D/A board. A more detailed description of the program created will be presented later in this chapter.

3.1.2 **Simulation Components**

Once the analog data had been generated and outputted from the computer it was sent to the test apparatus where the pressure pulses were simulated inside the intake manifold. This portion of the experiment consisted of two 500 watt MEI amplifiers used to boost the analog signal, four 4 inch speakers were used to transduce the signal into the manifold runners and the intake manifold being studied. The manifold used was a polypropylene constructed manifold used on the single cam Chrysler Neon engine. This manifold was chosen for its relatively simple geometry and for its availability of noise

and waveform data. An aluminum block was also constructed to act as an interface between the round speakers and the oval manifold runner openings. The block also incorporated an insulating enclosure around each of the four speakers so as to eliminate any acoustical influences between the speakers. Figures 3.1 and 3.2 illustrate the aluminum block mounted to the manifold with and without the insulating enclosure respectively.

3.1.3 Acquisition and Analysis Components

The equipment and instrumentation required for data acquisition and analysis include a microphone, an analog to digital input board and analysis software.

A Bruel and Kjaer type 4134 condenser microphone with a useful range of 20 Hz to 20,000 Hz was used to pickup the manifold signal at the throttle body of the intake manifold. The Electronic Instrument Master Catalogue by Bruel & Kjaer [1] can be examined for a more technical description of the microphone. The microphone was mounted using a clamping device which rigidly held the microphone at a selected position relative to the throttle body opening. The microphone signal was amplified with a Bruel and Kjaer Type 2606 measuring amplifier prior to being sent to the computer. This amplifier is further described in the B&K reference [1].

A National Instruments AT-A2150 dynamic signal acquisition board was used to digitize the microphone's analog signal prior to processing by the analyzer software. The AT-A2150 is capable of digitizing a signal with a bandwidth from DC to 20 kHz and was designed for applications including sonar, shock and vibration, noise audio, speech and

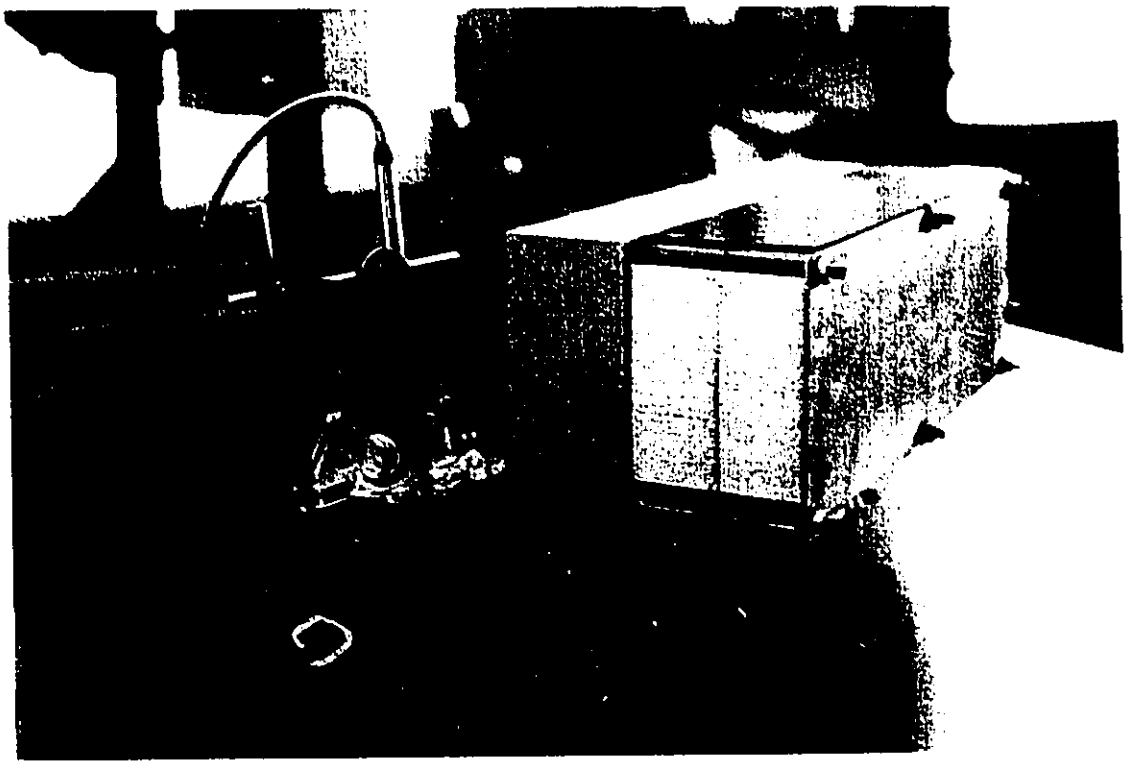

Figure 3.1: Manifold with Insulating Enclosure

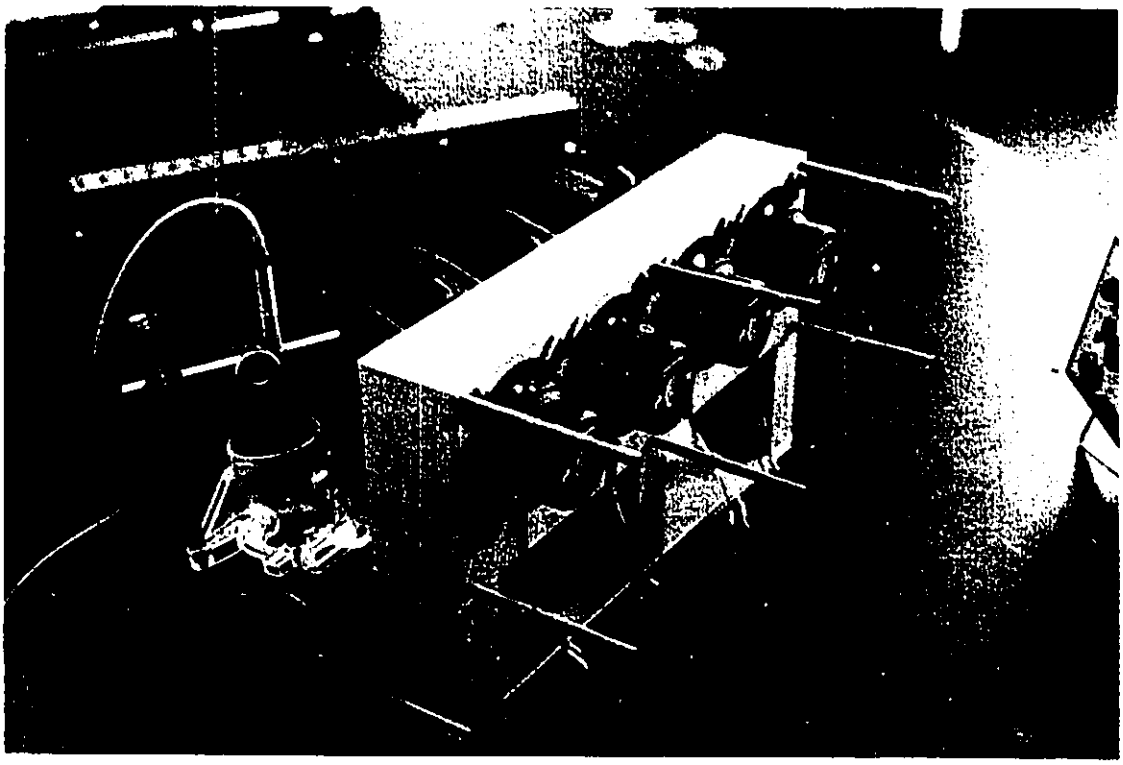

Figure 3.2: Manifold without Insulating Enclosure

acoustic testing and analysis. A more thorough description of the technical characteristics of the analog to digital input board can be found in the Appendix A or in the references [10][11][12].

Once digitized, the microphone signal was analyzed using a modified Dynamic Signal Analyzer software program created using National Instruments' LabView programming software. This analyzer is capable of displaying the signal in both the time and frequency domain.

A typical time domain signal is illustrated in Figure 3.3. This complete cycle shows the amplitude of the microphone's voltage signal over the time period required to complete one cycle.

The signal was also analyzed in the frequency domain as illustrated in Figure 3.4. The software utilizes the Fast Fourier Transform (FFT) algorithm to convert the input time domain signal into the frequency domain. The analyzer is capable of applying a number of outputs including amplitude spectrum, power and cross-power spectrum as well as impulse response. Additionally, different smoothing windows can be applied depending on the most appropriate application. All tests were done at a sampling rate of 612 with 25 averages taken. This was determined to be the most appropriate number resulting in a steady state output.

3.1.4 **Acquisition Components for Engine Tests**

Figure 3.5 illustrates the equipment employed to record the induction noise data produced by an operating Chrysler Neon. A Bruel & Kjaer type 4134 condenser

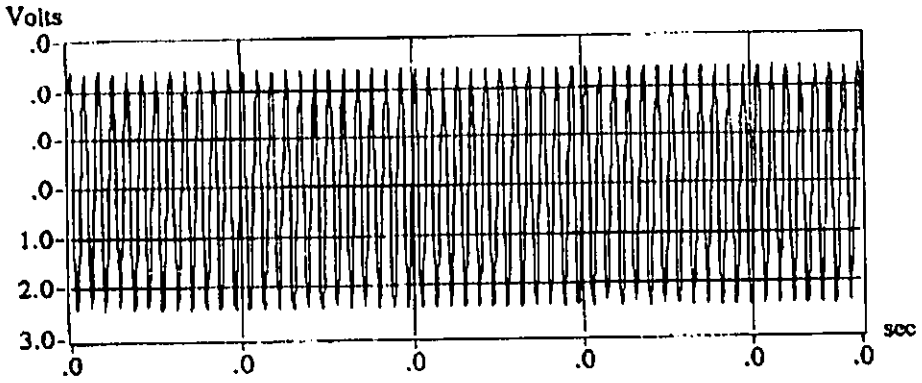

Figure 3.3: Typical Time Domain Signal

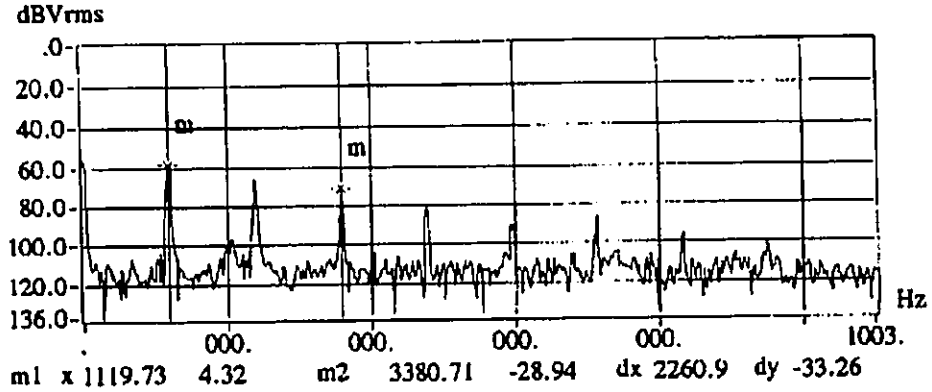

Figure 3.4: Typical Frequency Domain Signal

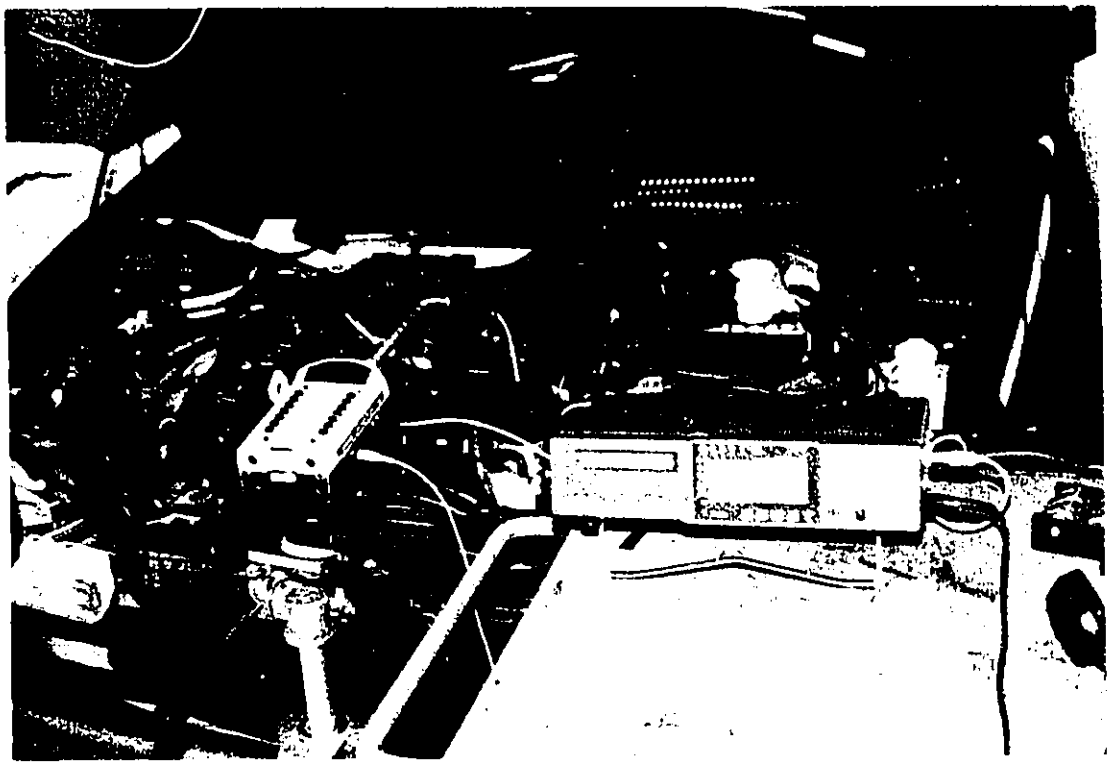

Figure 3.5: Equipment Used to Record Engine Data

microphone mounted on a B&K Type 2231 Sound Level Meter equipped with a BZ7101 Statistical Analyzer Application Module was used to record the produced intake noise at the throttle body. This signal was then stored on a Sony Digital Audio Tape recorder for future playback and analysis. All processing and analysis of the stored information was done with the National Instruments A/D board and analysis software as described previously in section 3.1.3.

3.2 Experimental Design and Preparation

In order to ensure the integrity and repeatability of the data collected, care must be taken in the design of the experimental setup. The following section describes how the different components mentioned earlier are combined to achieve the overall design configuration used to produce and collect reliable data.

3.2.1 Experimental Simulation Tests

The schematic diagram in Figure 3.6 illustrates the flow and interaction of the various components used in the experimental simulation and measuring tests. The fundamental components used to simulate the desired effects include the computer program and hardware used to produce the simulation data, the amplification device and speakers used to produce the pressure pulses along with the manifold and supporting structure under study. The fundamental components used to measure and analyze the data include the microphone and signal amplifier and the computer program and supporting hardware required for analysis.

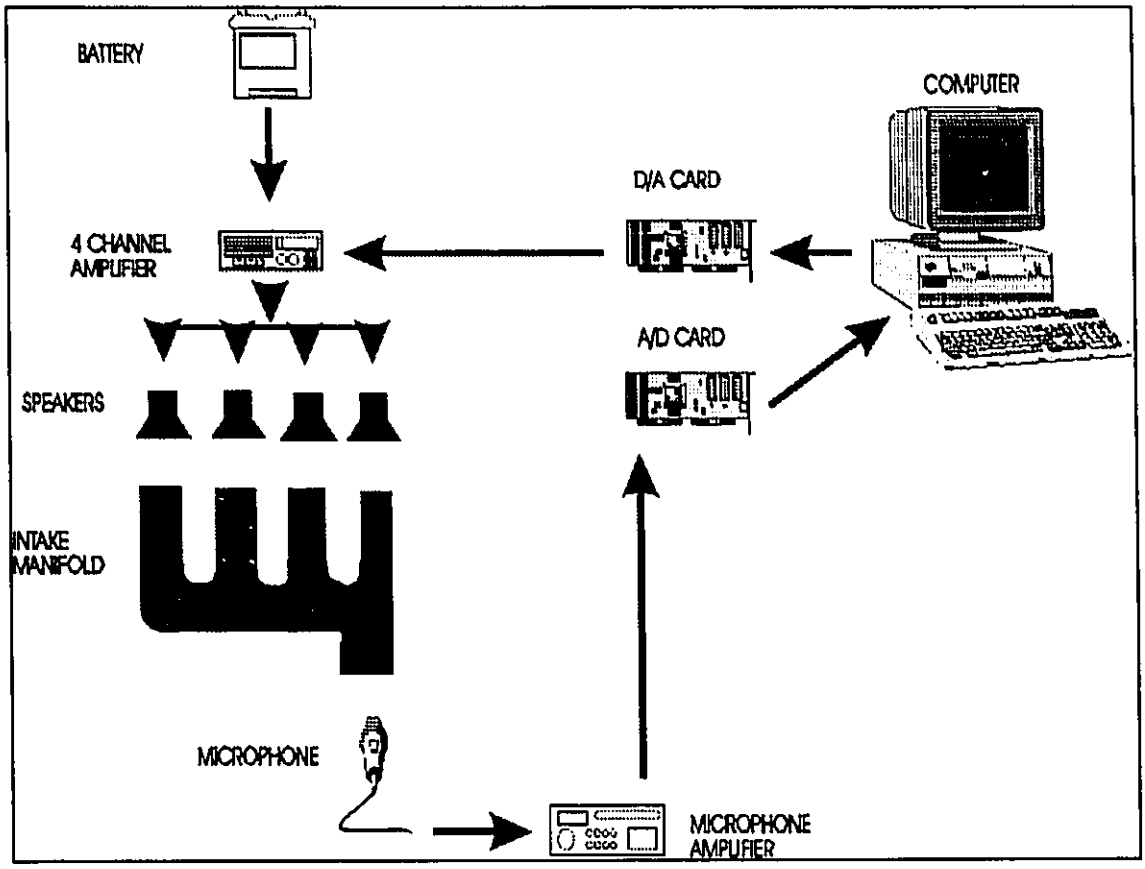

Figure 3.6: Schematic of Simulation Experiment

3.2.1.1 Software and Hardware For Simulation Data

As mention earlier, the pressure pulses generated in the manifold runners are derived from digital information acquired from the Ricardo Wave Model, a theoretical simulation model used by industry. A listing of this data has been included in Appendix B. This sample represents the pressure amplitude at the four runner openings versus the piston's crank angle at an engine operating speed of 2400 RPM.

In this simulation, the data, stored in a Quattro spreadsheet, is retrieved by a computer program which interfaces with the AT-AO-10 digital to analog output board. The controlling computer program was created using the graphical programming software package LabView. An illustration of the source code for the main program is given as Figure 3.7.

The initial functions of the program include the configuration of the output board, defining the buffer size to contain the data and providing an interface with the user. This interface allows the user to define some of the output board parameters such as device and channel identification. Figure 3.8 illustrates the user interface screen which controls the execution and operation of the program.

The program then retrieves the wave data from the four column matrix spreadsheet and stores it in the allocated buffer. The four columns represent each of the four channels of information which must be output from the A/D board with each channel representing one of the four engine cylinders. When ready, the program begins to write

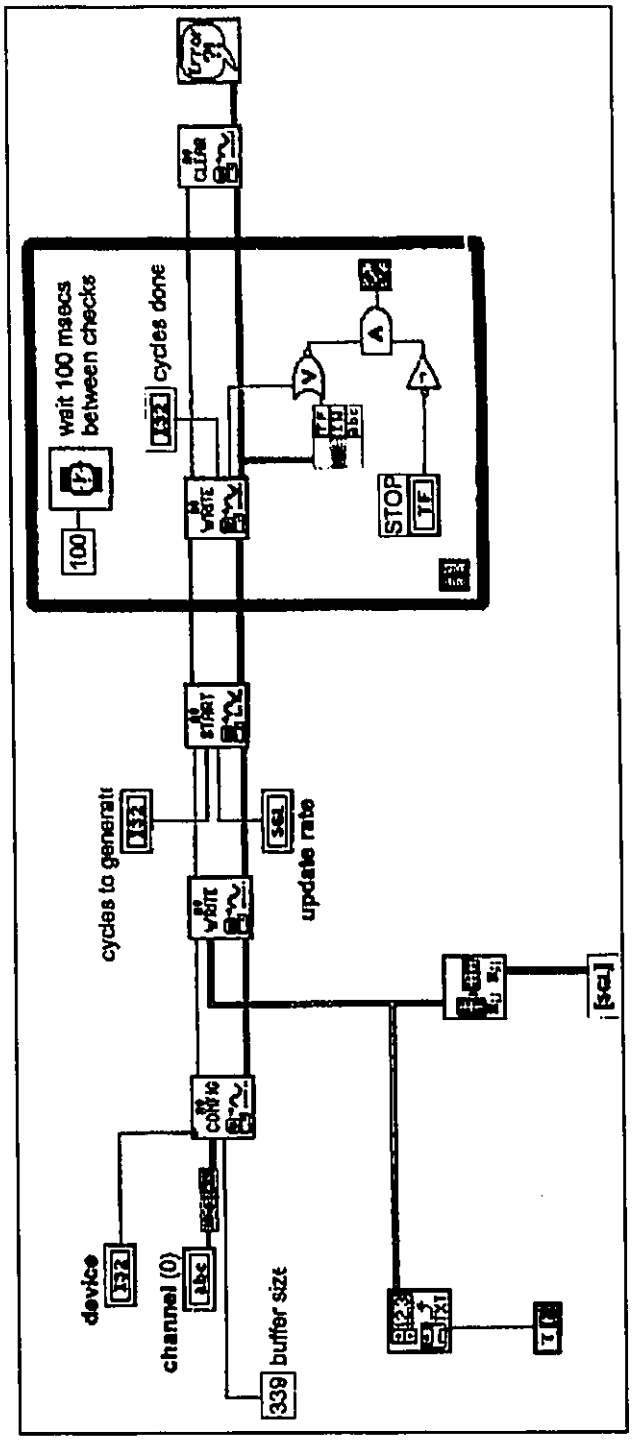

Figure 3.7: Source Code from Main Program

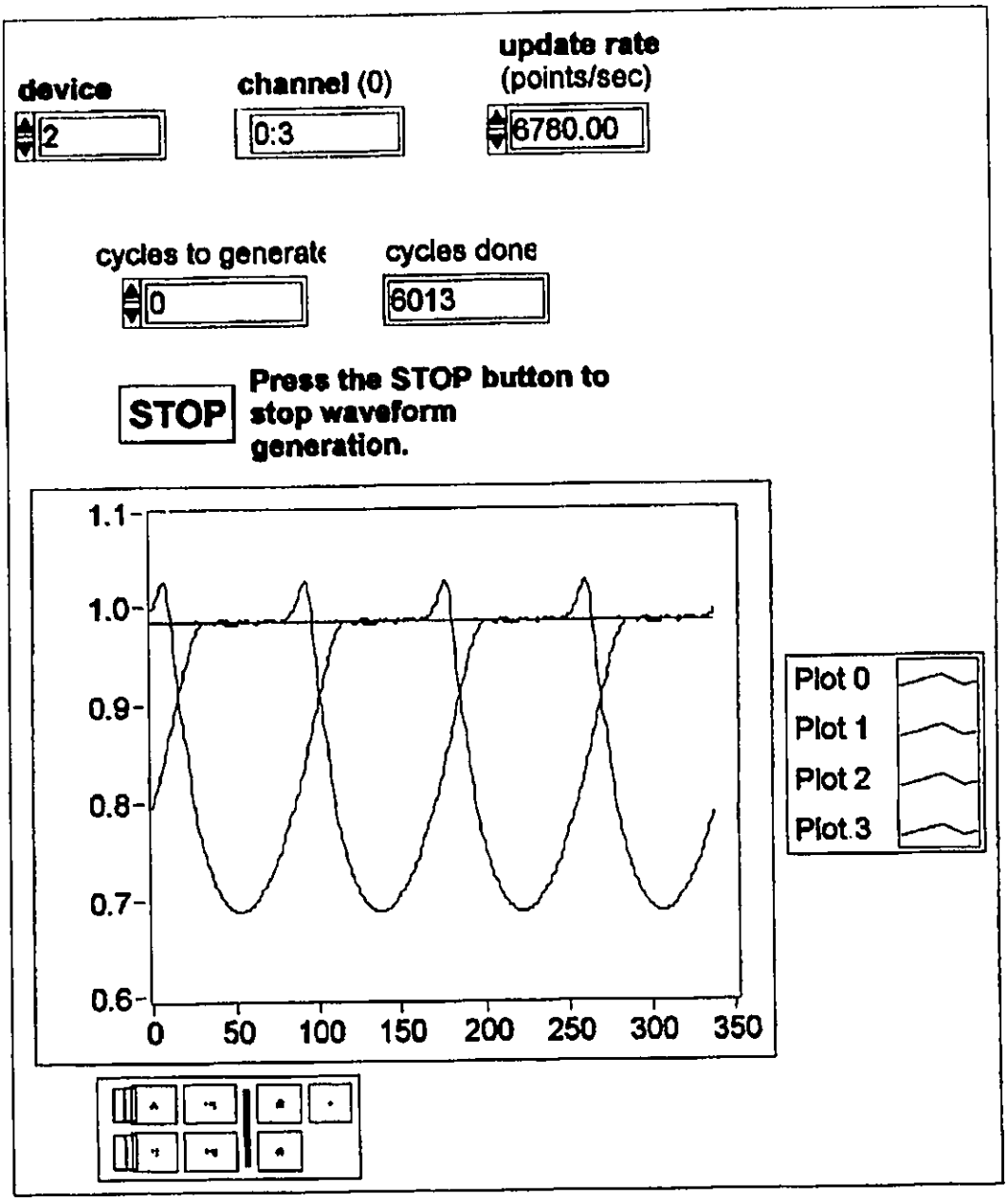

Figure 3.8: User Interface Display for Main Program

the data to the D/A board and user screen at the rate and number of cycles specified by the user. Once complete, the program re-initializes the board for the next run.

Many of the functions are carried out by subprograms as identified by the square boxes in the source code diagram. A description of the use of the subprogram components can be found in Appendix C or in reference [9].

Once the digitized information is sent to the output board, each of the four channels are simultaneously converted to a voltage signal proportional to the initial pressure information. This analogue signal is then sent to two dual channel battery powered amplifiers which boost the signal to a level suitable to drive the four speakers. It is these speakers which are interfaced with the manifold runners which mechanically reproduce the pressure information thus simulating the timed pressure pulses which propagate through the manifold.

3.2.1.2 **Software and Hardware Used to Analyze the Data**

The noise signal released through the throttle body opening is picked up by the microphone which is concentrically mounted 5 cm above the opening. The height of 5 cm was chosen to be consistent with industry standard tests and data [2][3]. This also provides a common reference permitting better correlation of results from other tests. The microphone output is then amplified and sent to the AT-A2150 dynamic signal acquisition board for digitization. Both the controlling of the acquisition board and processing of the measured data is administered by a second computer program, also created using LabView.

Figure 3.9 is an illustration of the graphical source code for the main portion of the analysis program. The primary functions associated with the main program are initializing and controlling the interface functions with the user and providing the platform for the analysis subprograms. Due to the complexity of this program, it is recommended that the reader refer to reference [9] for a more detailed description of the various operations associated with this program.

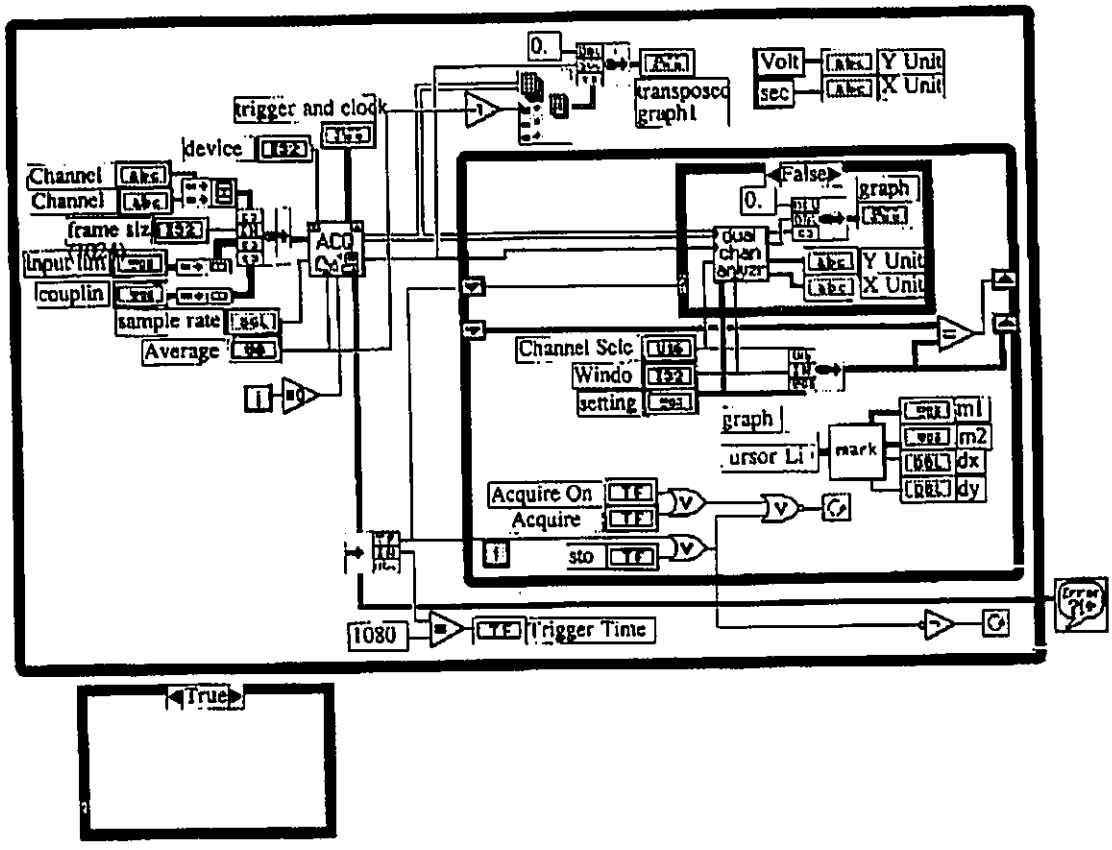

Figure 3.9: Source Code for Analysis Program

3.2.2 Operating Engine Tests

The fundamental components used in the testing and analysis of the manifold mounted on the operating engine include the intake manifold under study, the acquisition equipment used to record and store the data and the computer program and supporting hardware required for analysis.

All experimental tests were performed on an intake manifold mounted on a 1996 model year Chrysler Neon. The vehicle was mounted on a dynamometer as shown in Figures 3.10 and 3.11. Figure 3.10 shows the vehicle mounted on the dynamometer complete with noise attenuation shields to minimize any potential tire noise impact on the measurements being made. Figure 3.11 illustrates the dynamometer control room which controls and monitors the operations of the dynamometer and subsequently the automobile and engine being tested. The dynamometer allowed for the tests to be performed under conditions which most simulate every day operating conditions by including the interaction with all other engine components with the vehicle under loading conditions similar to those found on the road.

Once the engine was brought to steady state conditions at the desired RPM, the measurements were made using the Bruel & Kjaer microphone and sound level meter. It should be noted that the microphone was mounted at the same position above the throttle body opening as it was during the experimental simulation tests done on the test bench. The position of the microphone is illustrated in Figure 3.12. The signal was then taken from the sound level meter and recorded on a digital audio tape.

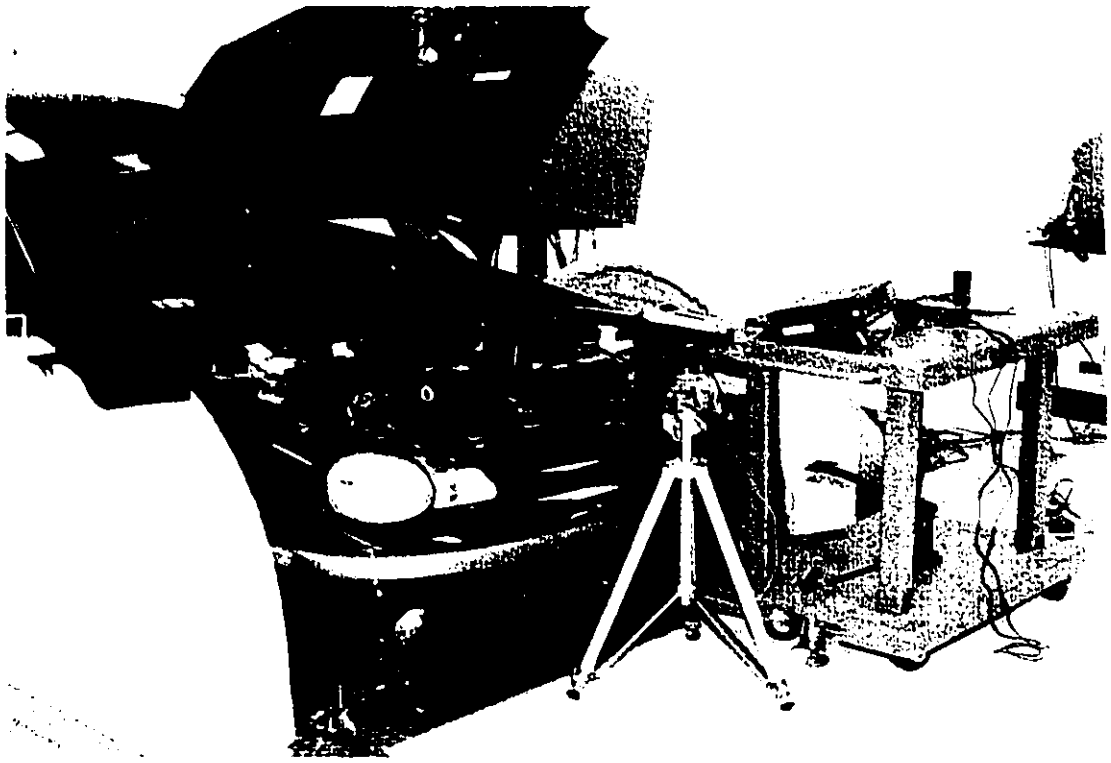

Figure 3.10: Vehicle Mounted on Dynamometer

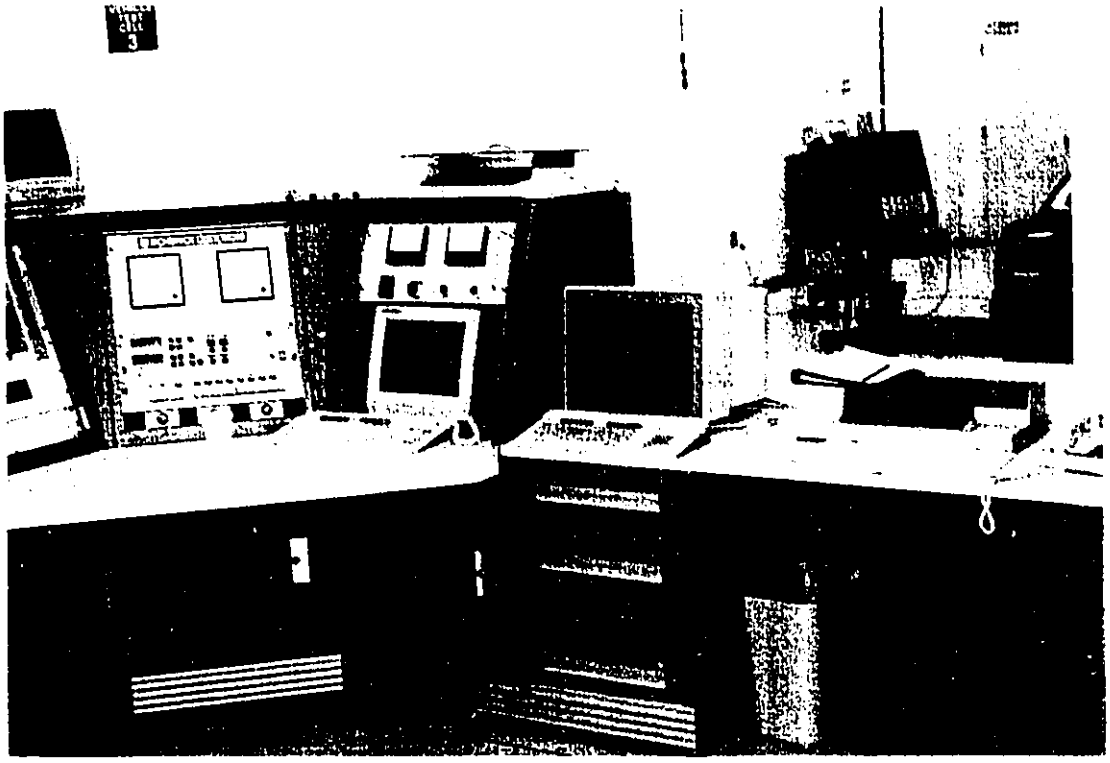

Figure 3.11: Dynamometer Control Room

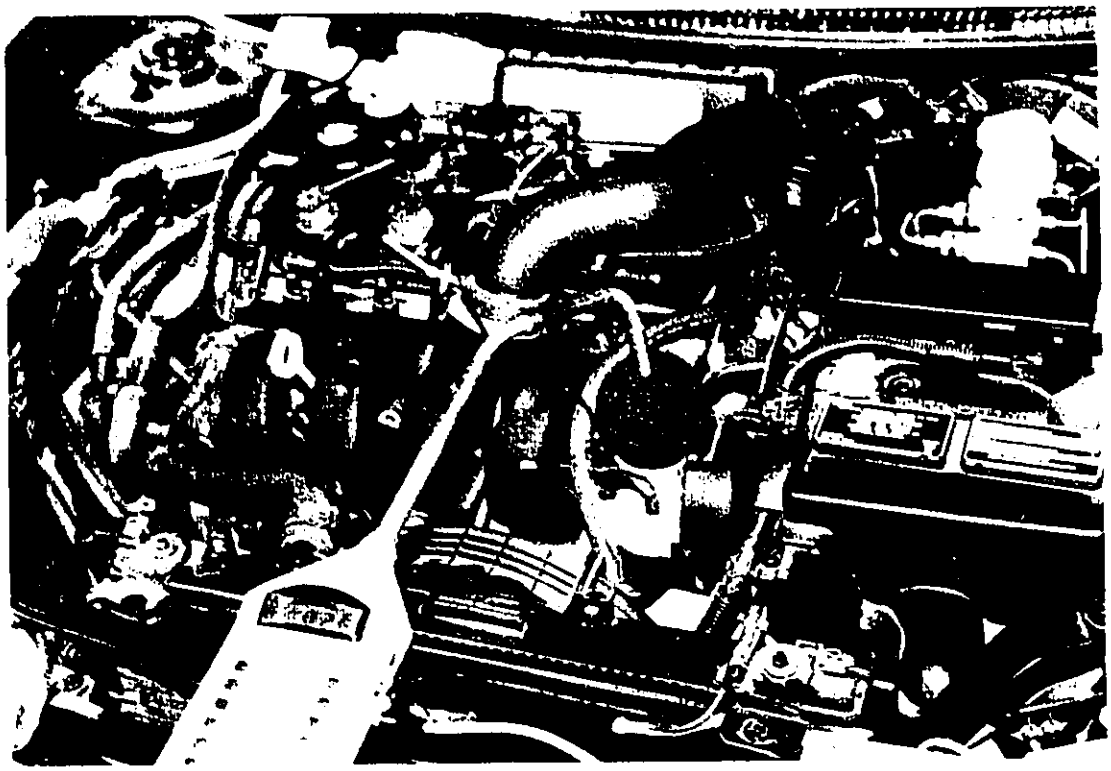

Figure 3.12: Microphone Position

Once all tests were recorded on the digital tape, the DAT recorder was connected to the AT-A2150 dynamic signal acquisition board and computer for analysis. From this point, the procedure for analysis of the recorded information is the same as that for the simulation tests as described previously in section 3.2.1.2.

3.3 Experimental Procedure

The steps taken to generate the simulated pressure pulses in the experimental manifold and simultaneously acquire and analyze the noise data at the throttle body are outlined in the following section. Also given below is the process used to acquire the intake noise data from the operating engine.

3.3.1 Simulation Tests on Experimental Manifold

The following is a step by step procedure outlining the steps taken to generate and analyze the data for the experimental manifold simulation:

1. Develop the experimental model and purchase and/or manufacture any required supporting elements.
2. Create the computer program using LabView that will read a pressure data file, configure the D/A output board, and write the data to the output board to be converted to a voltage signal.
3. Create the computer program using LabView that will accept the acquired noise data from the A/D input board and display the time and frequency content of the measured signal for analysis.
4. Obtain manifold runner pressure versus crank angle data from the Ricardo Wave program and store in a file format suitable for retrieval by the LabView generation program.

5. Obtain manifold throttle body noise data from the Ricardo Wave program for future comparison with measured data from the experimental model.

6. Execute the generation program to simulate the pressure pulses in the intake manifold for an engine operating speed of 2400 RPM.

7. Acquire data with microphone at five cm from throttle body, amplify the signal and send to the input card for digitization.

8. Process the acquired data and output the time and frequency content of the noise signal.

9. Do a comparison of the acquired time signal to the time signal as specified by the Ricardo Wave Model. Quantitatively compare the fundamental frequencies of the acquired experimental data to the frequencies as specified by the Ricardo Wave Model.

3.3.2 Actual Tests on Operating Engine

The following is a step by step procedure outlining the steps taken to acquire and analyze the data for an intake manifold on an operating engine under load:

1. Drive automobile onto dynamometer and prepare vehicle for loading tests. Remove air cleaner and ducting from automobile engine and mount microphone five cm above throttle body opening.

2. Bring vehicle to test speed under load such that engine RPM is at 2400.

3. Acquire noise data with microphone and store on digital audio tape for future analysis.

4. Retrieve stored noise signal and send to the input card in computer for digitization. Process the acquired data and output the time and frequency content of the noise signal.

9. Do a comparison of the time signal from the operating engine to the time signal as specified by the Ricardo Wave Model and the time signal from the simulation experiment. Also quantitatively compare the fundamental

frequencies of the acquired data from the operating engine tests to the frequencies as specified by the Ricardo Wave Model and the fundamental frequencies from the simulation experiment.

IV. ANALYSIS OF DATA

The most important step in developing a simulation model is collecting the appropriate data required to compare the simulated data to the known benchmarks. Two types of data were used for correlating the simulation results to the other data sources. These two types being time domain information and frequency domain information. In this chapter, the fundamental concepts describing the two data types will be separately explored along with a description of the measurement and analysis procedures used.

4.1 Data Analysis

The first step in analyzing the noise data involves either the playback of the stored Neon engine noise data from the DAT recorder or the real time data measurement from the simulator model. This information is digitized and fed into the LabView analysis program. Special attention must be given to the conversion process from analog to digital. Specifically, the rate of data sampling must be carefully considered as well as proper calibration of the signal.

4.1.1 Sampling

Sampling is the process of representing a continuous time record or wave by a number of discrete equi-spaced points. Figure 4.1 illustrates a continuous analog wave that has been represented by a number of equally spaced points. The interval between points, defined by 'h' in the figure is the sampling interval and must be chosen carefully.

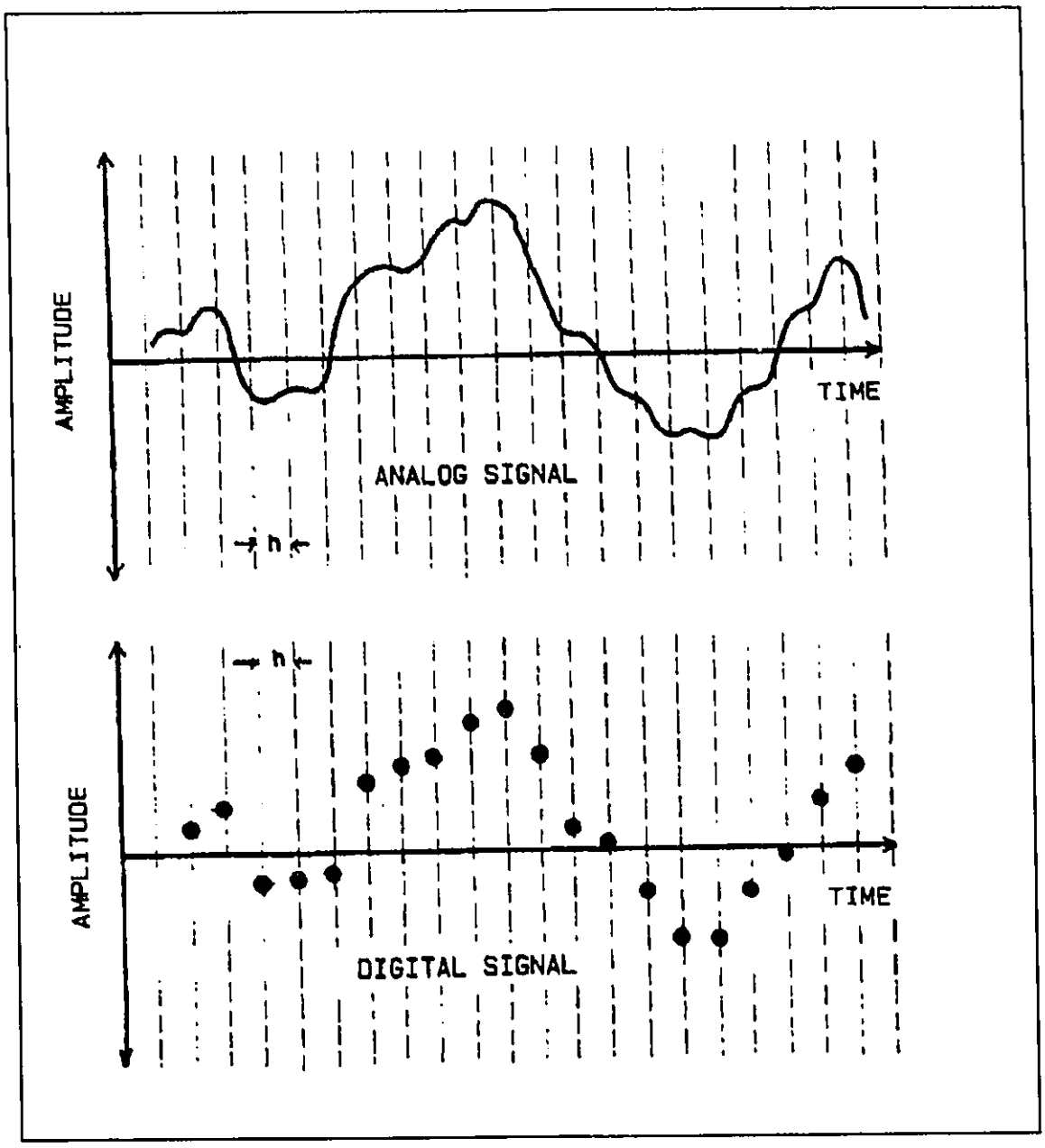

Figure 4.1: Sampling Process of Analog Signal [4]

If too small an interval is chosen, the time record will be represented by more data points than are required. This redundancy of data results in an unnecessary increase in time and labour in processing of the data. If too large a sampling interval is used, the high frequency components, that is, the frequencies above half the sampling frequency, are misinterpreted as lower frequencies. This phenomenon is referred to as aliasing and must be avoided when digitizing continuous signals. A common example of aliasing is illustrated by the backward movement, or negative frequency, of wagon wheels in western movies because of the sampling involved in the filming [19]. In order to eliminate the adverse effects of aliasing, the Nyquist theory postulates that the sampling rate required for digitization should be no less than 2.56 times the highest frequency of the original data acquired [20].

4.1.2 **Calibration**

In the analysis of the acquired signal, it may be desirable to express the results directly as an amplitude spectrum where the amplitudes have the same dimensions as the input signal [19]. In order to accomplish this, a reference, or calibration signal, is digitized and recorded before and/or after the data is digitized. Reference to this calibration signal is then made later to determine the relationship between the digitized units and the physical units. For this study, a calibration signal of 1000 Hz and 93.8 dB was recorded prior to the acquisition of all data. Figure 4.2 illustrates the LabView output for the calibration signal recorded prior to the acquisition of data for the pulsation simulator model. Given this information, the voltage measured for both the simulated

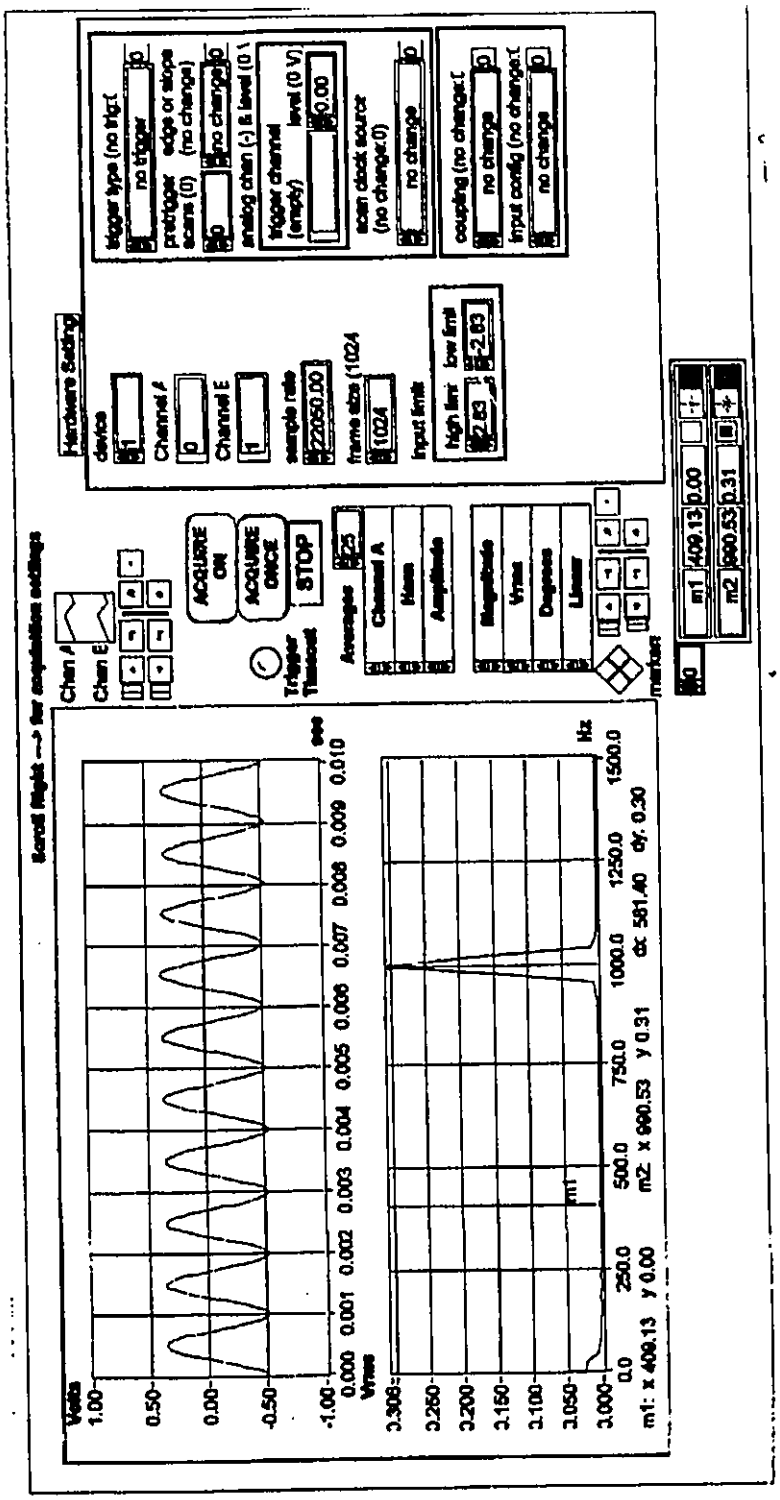

Figure 4.2: Calibration Signal For Simulation Measurements

and actual intake data can be directly related to the amplitude units provided by the calibrator unit.

4.2 Time Domain Signal

As mentioned at the beginning of this chapter, two types of data will be used to correlate the data measured from the simulation model to the theoretical and actual Neon engine data. The first type, being time domain data, will be discussed in this section.

4.2.1 Classification of the Measured Signal

The type of signal to be analyzed has an influence on the type of analysis to be carried out [19]. For a stationary signal, that is, a signal whose average properties do not vary with time, it must be established whether the signal is deterministic or random. For a deterministic signal, a given instantaneous value is easy to predict at all points in time. In other words, the signal can be described by some explicit mathematical function as illustrated in Figure 4.3. Random signals on the other hand, can not be described by an explicit mathematical function. Stationary random signals can only be described by their statistical properties such as the mean values, variances etc.

Figure 4.4 illustrates a typical measurement at the throttle body of the Neon engine. The graph shows the measured signal in the time domain. From this, it is obvious that the signal belongs to the non-determinate, or random category. Therefore, the characteristics of the signals in this study had to be described using statistical functions in addition to qualitative descriptors. For this purpose it was decided that mean value,

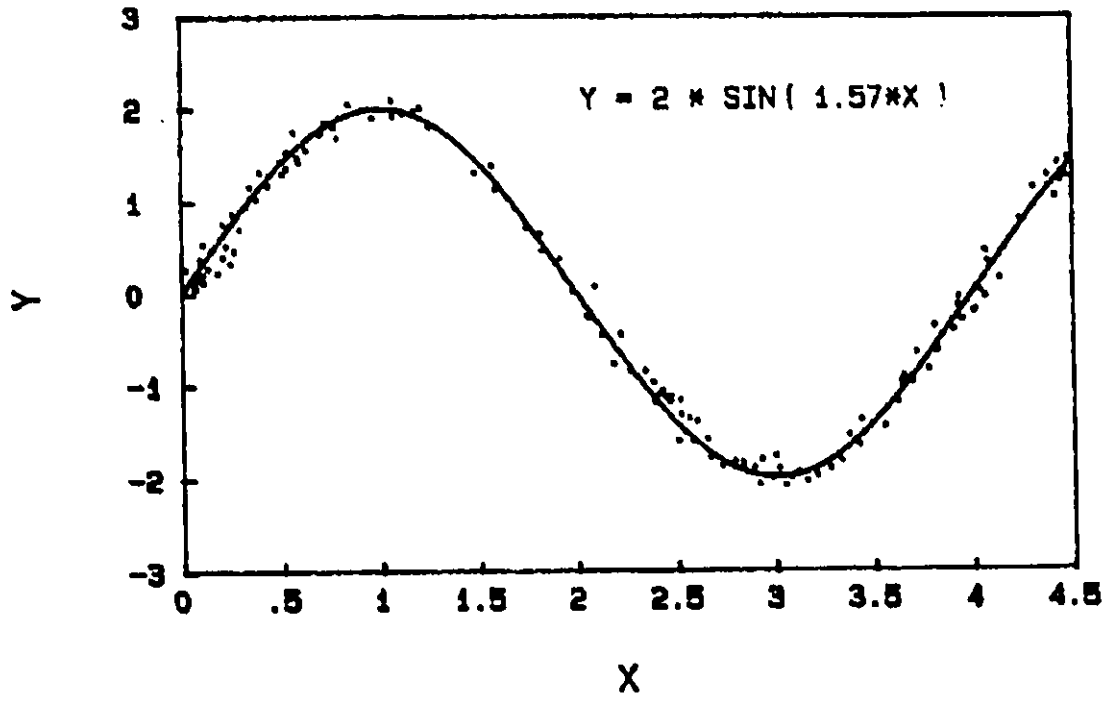

Figure 4.3: Deterministic Data [4]

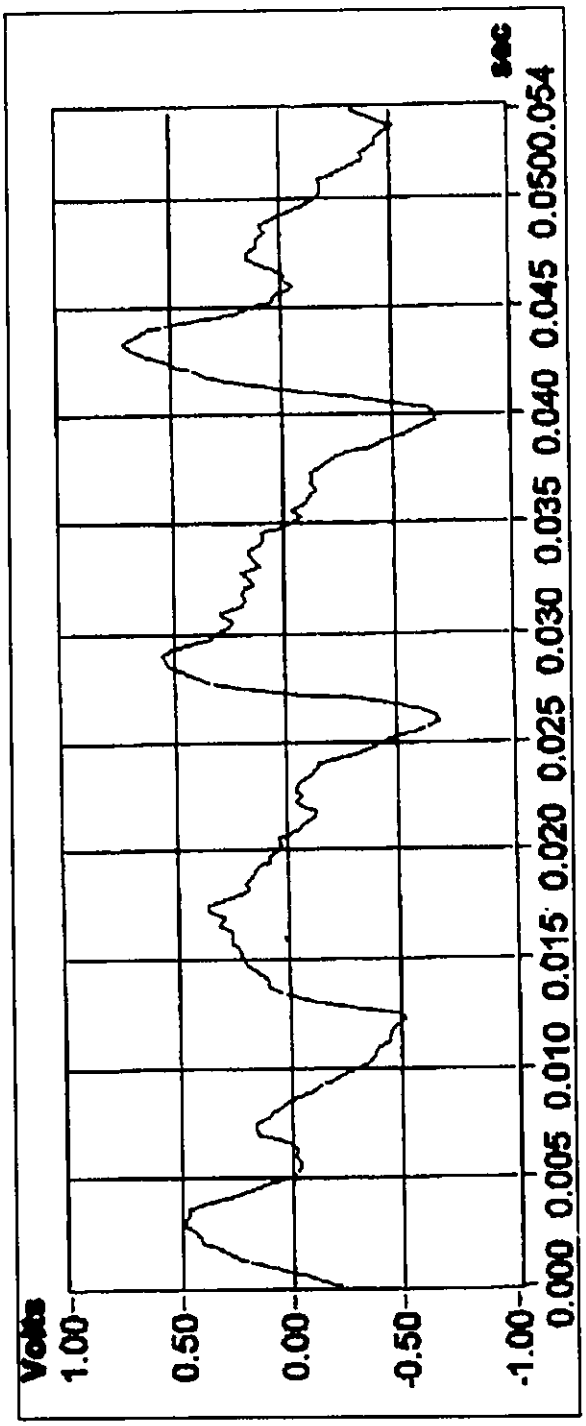

Figure 4.4: Time Domain Output For Neon Engine

standard deviation, correlation coefficient and covariance be used to compare the simulated data points to the actual data points measured on the operating Neon engine. This exercise is not possible with the theoretical time domain curve since the data describing this curve was not available. A plot of the theoretical time domain is, however, available thus allowing for a qualitative comparison to be made. This qualitative analysis will also include the plots from the simulated and actual time domain analysis.

4.2.2 **Statistical Descriptors**

The following is a description of the statistical parameters that were used to compare the data points from the experimental model to the actual data points measured on the operating Neon engine. A more detailed description can be found in the references [7][15].

4.2.2.1 **Mean**

The mean of a set of data is a measure of the centre of the set in the sense of an average. That is, observations usually group themselves about a central value. The measurement of this central tendency is described as the mean denoted by the Greek letter μ (mu). The mean is also described as the first moment about the origin.

4.2.2.2 Standard Deviation

Quantification of the dispersion, or degree of clusterness of a set of data about the mean is defined as the variance, also known as the second moment about the mean. However, the dimension of variance is in square units which are not the same dimension of the random variables. This can be adjusted by taking the square root, thus defining the standard deviation which is denoted by the Greek letter σ (sigma).

4.2.2.3 Correlation Coefficient

Determination of the correlation coefficient quantifies the correlation between the numeric values in two or more sets of data. Correlation coefficients range in value from -1.0 to 1.0. A set of data correlated with itself returns a correlation coefficient of 1.0 whereas a correlation coefficient of zero means that the two sets are not correlated [15]. The correlation coefficient is depicted by ρ (rho).

4.2.2.4 Covariance

Another analysis tool used to compare two or more sets of data is the determination of covariance. A positive covariance indicates that as the values increase in one set of data they also increase in the other. That is, the sets move together. A negative covariance indicates that as the values in one set of data increase, they decrease in another. Here the sets move apart. Unrelated data sets have a covariance approaching zero [15].

4.3 Frequency Domain Signal

The second type of data used to correlate the data measured from the simulation model to the theoretical and actual Neon engine data is from the frequency domain. The fundamental basis of frequency analysis is the Fourier Transform which can take different forms. For this study, the Fast Fourier Transform (FFT) is employed for the purpose of deriving the measured signal contents into the frequency domain. Figure 4.5 illustrates a typical measurement at the throttle body of the Neon engine. This diagram shows the measured signal in the frequency domain.

4.3.1 Fast Fourier Transform

The Fast Fourier Transform has become a widely accepted diagnostic tool in such areas as the detection of misalignment and out of balance of mechanical systems, preventative maintenance and noise quantification to name a few. The Fast Fourier Transform accomplishes these tasks by breaking down a complex measured signal into separate components at various frequencies. Once isolated, these frequency components provide a unique signature characteristic useful for problem solving diagnostics and signal source identification. The latter of which was employed in this study for comparing the frequency contents of the various sources of induction noise.

4.3.1.1 Mathematical Properties of the FFT

The Fast Fourier Transform is an alternative calculation procedure to obtain the Discrete Fourier Transform (DFT). The implementation of the FFT algorithm results

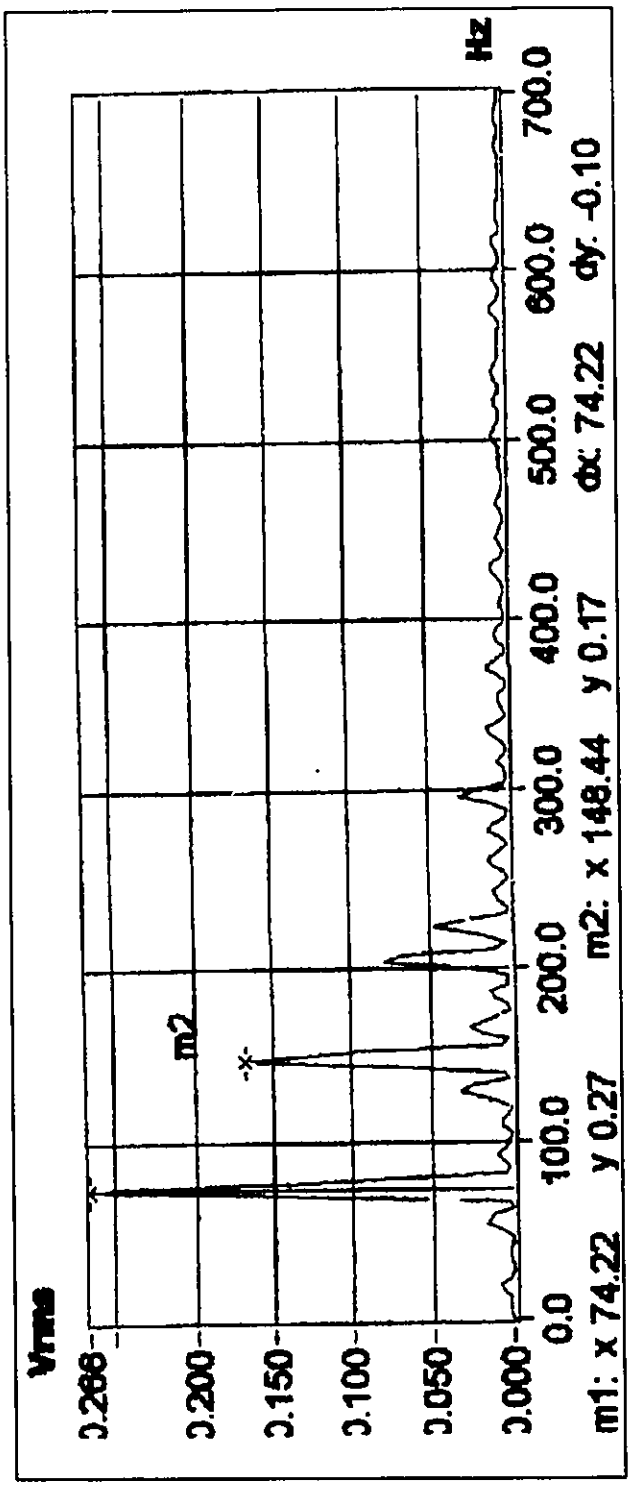

Figure 4.5: Frequency Domain Output For Neon Engine

in the identical final answer as the DFT with a greatly reduced number of arithmetic operations. Once a time signal has undergone an FFT process, the signal is represented by a vector in which each value represents the magnitude of the signal's frequency over the range of frequency values given in the vector. This is usually illustrated in graphical form. For a detailed technical explanation the reader is encouraged to consult with the references [8] [19].

4.3.1.2 **Limitations of the FFT Process**

While the FFT process provides an efficient means of determining the frequency content of a time signal, precautions must be taken to avoid three common pitfalls, these being aliasing, leakage and picket fence effect.

As explained earlier, aliasing is the misrepresentation of higher frequency information due to an inadequate sampling rate. To eliminate this problem, care must be taken to ensure that the sampling rate be a least 2.56 times greater than the highest frequency of interest within the data. Alternatively, a low pass filter may be employed to eliminate the frequencies measured greater than half the sampling rate.

Leakage, also known as 'side window effect' and 'sidelobe generation', is the result of the time limitation necessary to fit the time signal into a finite record length. The effects of leakage can be combated through a technique called windowing. A thorough description of leakage and windowing can be found in the references [8][19].

The third effect, as illustrated in Figure 4.6 is known as the picket fence effect. Since it is not possible to represent the continuous spectrum of a signal, it must be

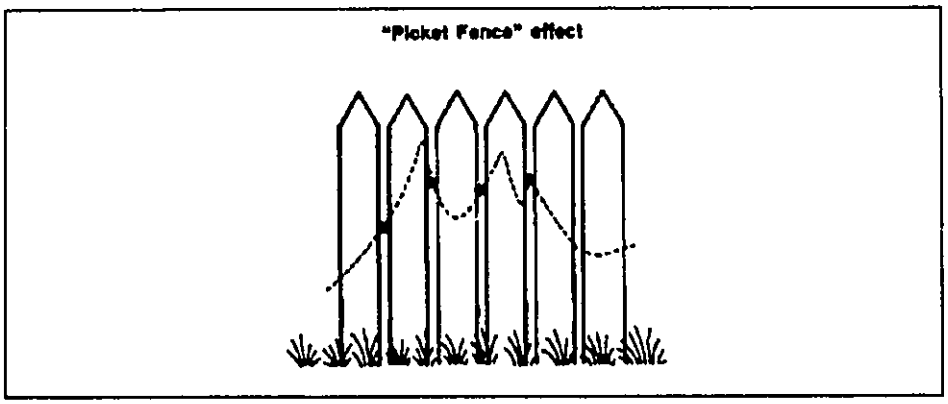

Figure 4.6: Illustration of Picket Fence Effect [19]

sampled discretely, much like looking through the slits of a fence. As a result, "the discrete sampling in the frequency domain corresponds to a periodic repetition of the time record with the period equal to the record length" [19].

4.3.2 **Time Domain Averaging**

Most stationary signals are comprised of three fundamental components being the periodic, semi-periodic and noise components [7]. For the purposes of this study, it is the periodic component that is desired, therefore, any spurious components must be eliminated from the original signal. This is accomplished by time domain averaging (TDA) which is accomplished by averaging the same data point within several time traces, thus producing an average time trace. Figure 4.7 illustrates the effect of two different averages performed on a stationary random signal.

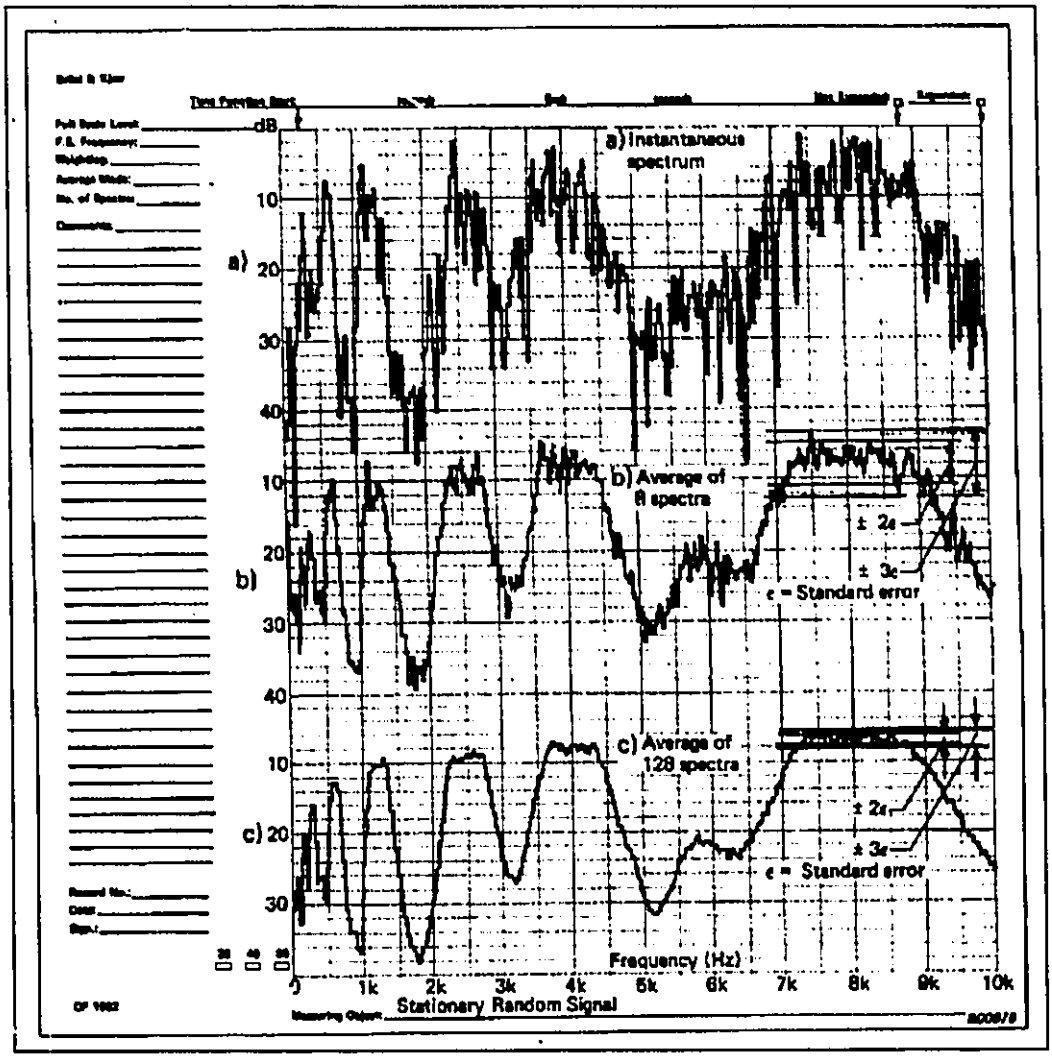

Figure 4.7: Effect of Averaging on a Stationary Random Signal [19]

V. DISCUSSION OF RESULTS

The results presented in this chapter compare the measurements amassed from the simulation model to the same measurements performed on both the actual Neon engine and to the outcome as predicted by the theoretical Ricardo Wave model. The data used to make these comparisons include the input data produced by the simulation model as well as the output noise signal as manifested at the throttle body opening.

5.1 Input Signal

The input signals that are presented here for comparing are from the Ricardo Wave model and from the simulation experiment. The theoretical data was derived by connecting a theoretical anechoic termination at the signal source. This allowed for the determination of the input signal without alterations from any other potential influences. It is not possible in the real world to perform the same experiment on the actual Neon engine and compile the same type of data. As a result, the comparisons of input data are restricted to the theoretical and simulated data sources.

Input data, that is, the data that enters the intake manifold runners at the manifold/engine head interface, was derived theoretically using an anechoic termination as described above. This input data, or pressure information, is caused by the pressure pulses resulting from the opening and closing of the intake valves as was described in the introduction of this thesis. Assuming that each of the valves are identical, the pressure

data is the same at each runner interface. Figure 5.1 illustrates the theoretical input data for one runner as determined by the Ricardo Wave model.

The theoretical data was input into the LabView program for signal generation via a spreadsheet file. Figure 5.2 illustrates the generated LabView signal for one runner.

Since the generated data was directly obtained from the theoretical Ricardo data it was felt that a qualitative evaluation of the two wave signals would suffice for the purposes of this study. This is reinforced by the fact that the principal focus of this thesis is on the resulting output waves at the throttle body and analysis of the input data is included only for thoroughness.

Given the above, it is explicit that the two input signals are the same. They have the same amplitude, duration and overall characteristic shape. This provides a high enough level of confidence in the input data to proceed with the analysis of the resulting output signals. It should be noted that the above referenced curves are representative for one manifold runner. Figure 5.3 shows the wave information for all four runners simultaneously. It is obvious that the four curves are identical in all respects except for phase. This is representative of the firing order for the engine which for the Neon is cylinders 3,4,2,1 respectively [3].

5.2 Output Signal

As was described in the previous chapters, the output signal was taken to be the resultant signal determined five centimetres up from the throttle body opening. Also, the analysis performed on the output signals were from two different data types. The results

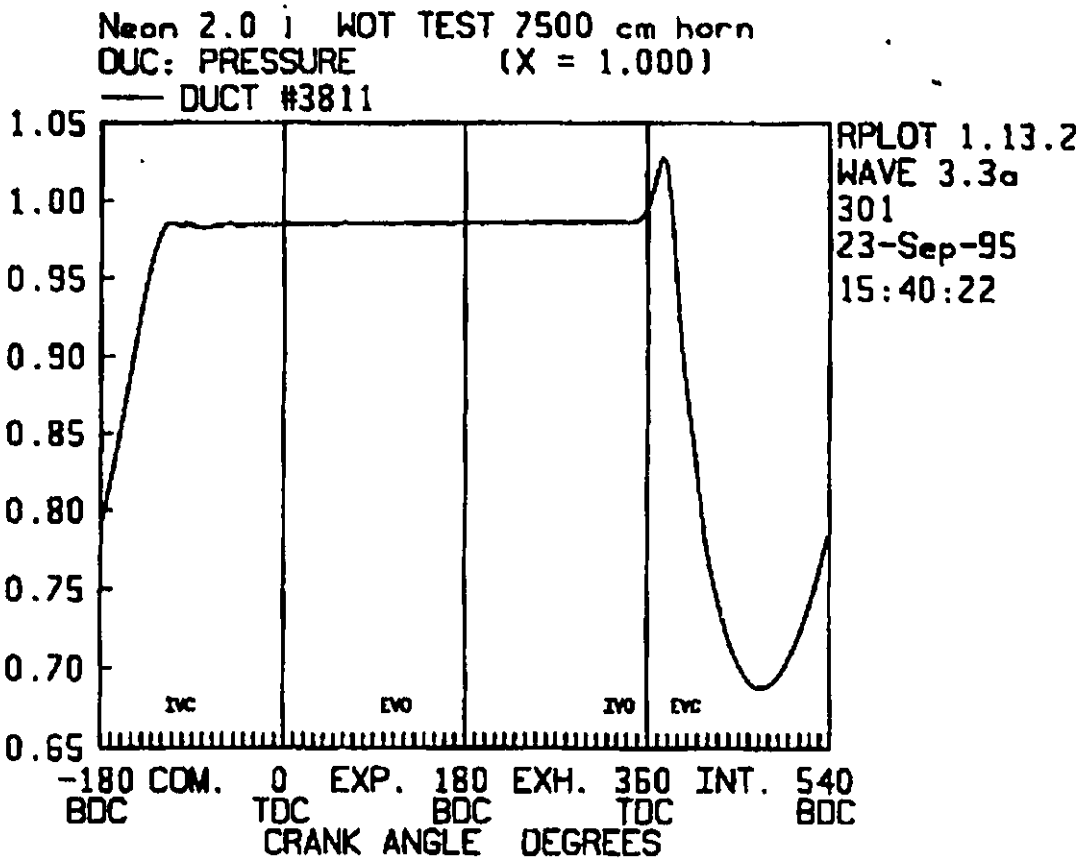

Figure 5.1: Theoretical Input Pressure Wave

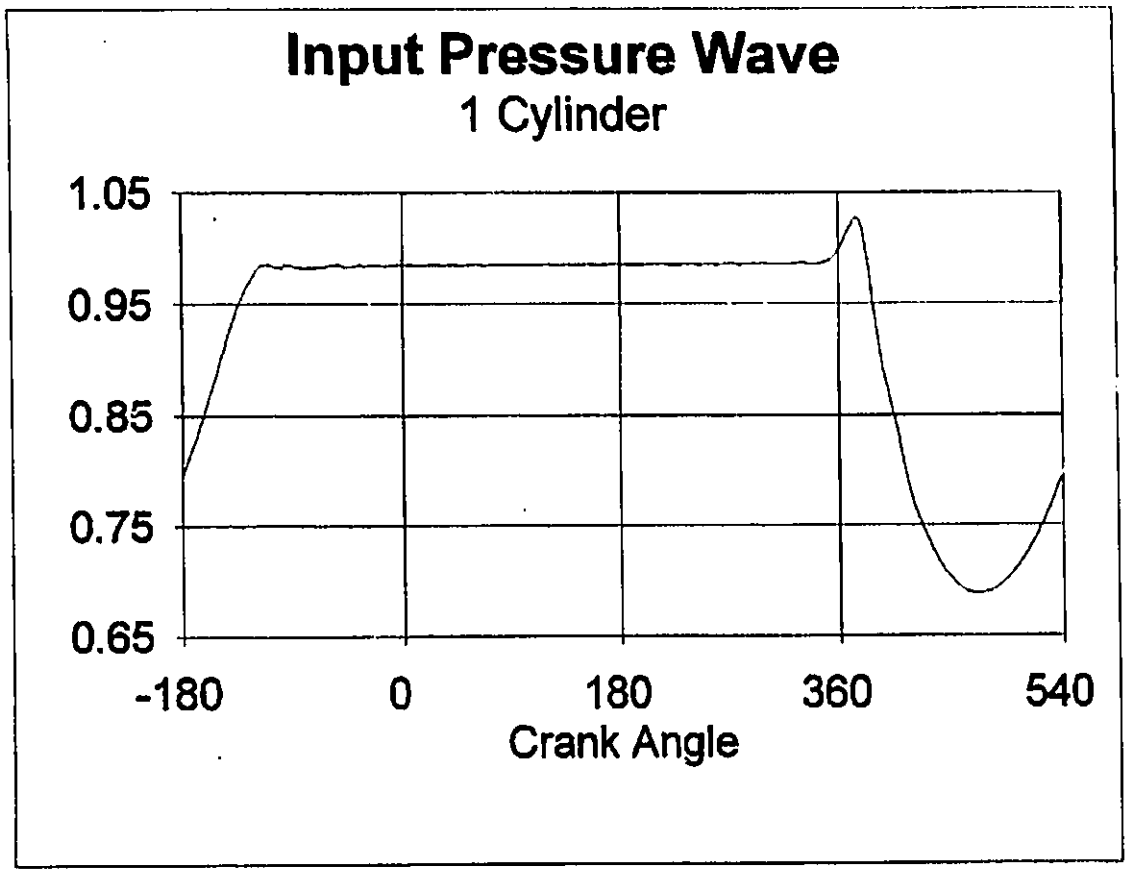

Figure 5.2: Experimental Input Pressure Wave

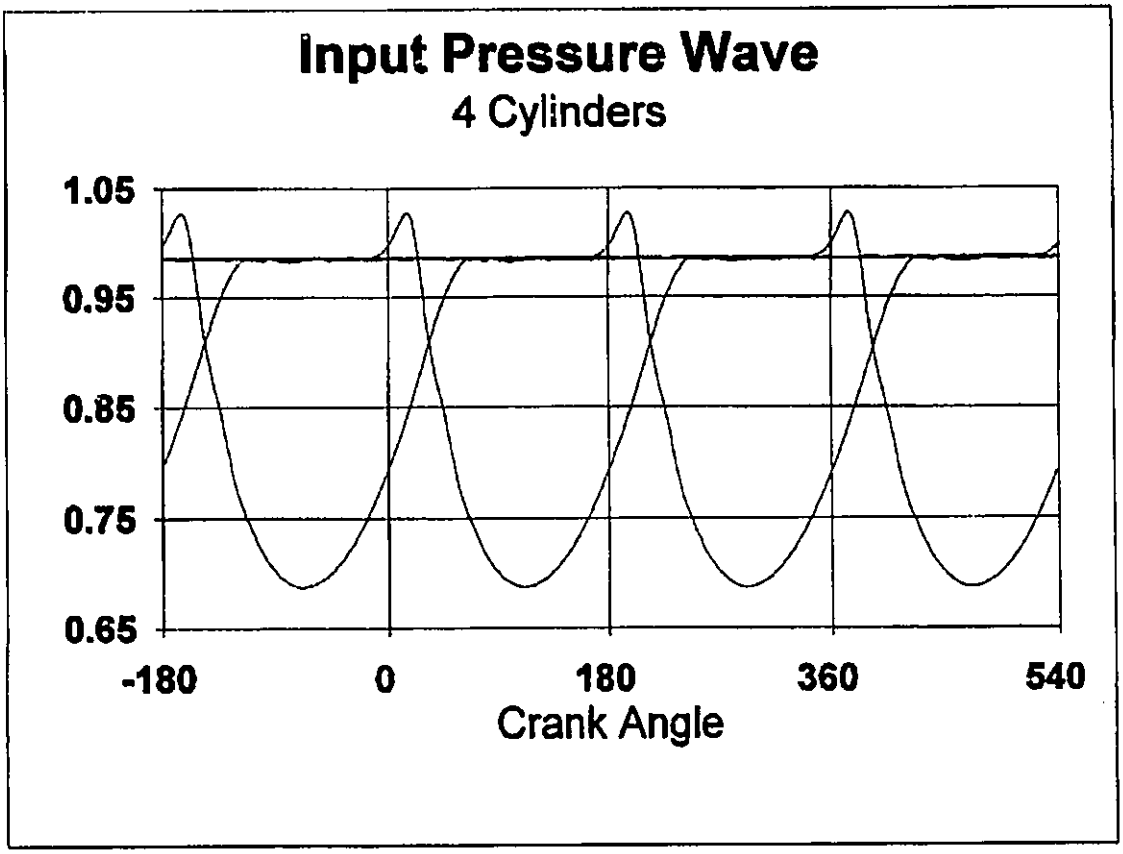

Figure 5.3: Experimental Input Wave for Four Cylinders

of the two data types, being the time domain and the frequency domain, are individually outlined below.

5.2.1 Results of Time Domain

The theoretical amplitude versus time output as predicted by the Ricardo Wave model is illustrated in Figure 5.4. The time axis has been represented by the crank angle degrees for one complete combustion cycle instead of seconds. It should be noted that the 720 degrees required for one combustion cycle consumes approximately 0.05 seconds.

Figure 5.5 illustrates one complete cycle for the amplitude versus time output for the measurements made on the Neon engine. This figure also shows that the combustion cycle encompassed a duration of 720 degrees, however, although not shown in the figure, it should be noted that the time duration for this cycle was approximately 0.054 seconds. The duration increase of 0.004 seconds was due to inaccuracies in maintaining a speed of 2400 RPM with the dynamometer. However, upon examination of the theoretical and actual time outputs, it can be concluded that they both possess the same general shape. This includes having the same characteristic peaks and troughs occurring at approximately the same position with respect to crank angle. The two outputs also display characteristic sub-peaks following each of the four major summits. Again, these appear to position themselves at the same locations with respect to the crank angle. Given this, it can be reasonably concluded that the time response results for the theoretical and actual engine tests correlate with a considerable degree of confidence.

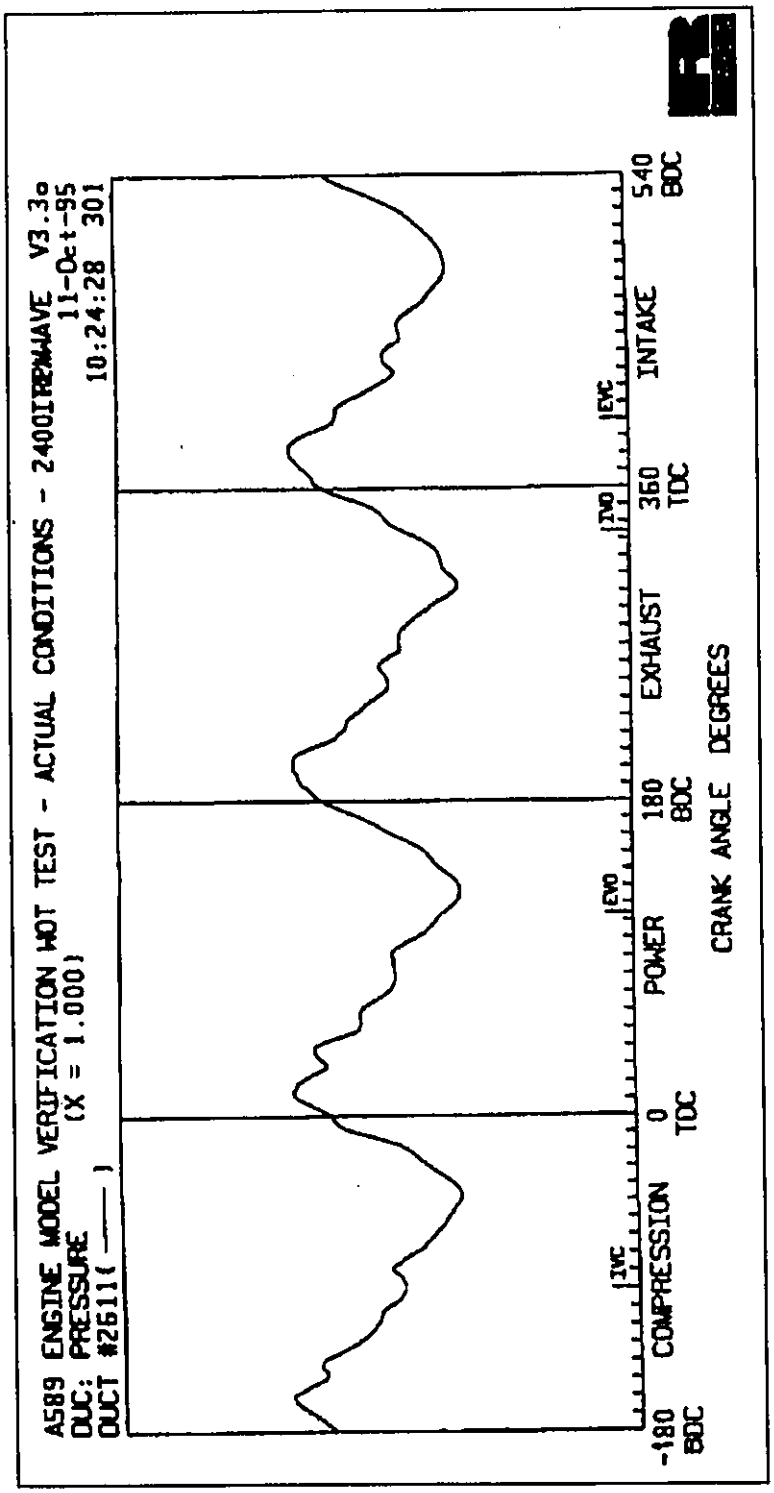

Figure 5.4: Time Domain Analysis for Theoretical Signal

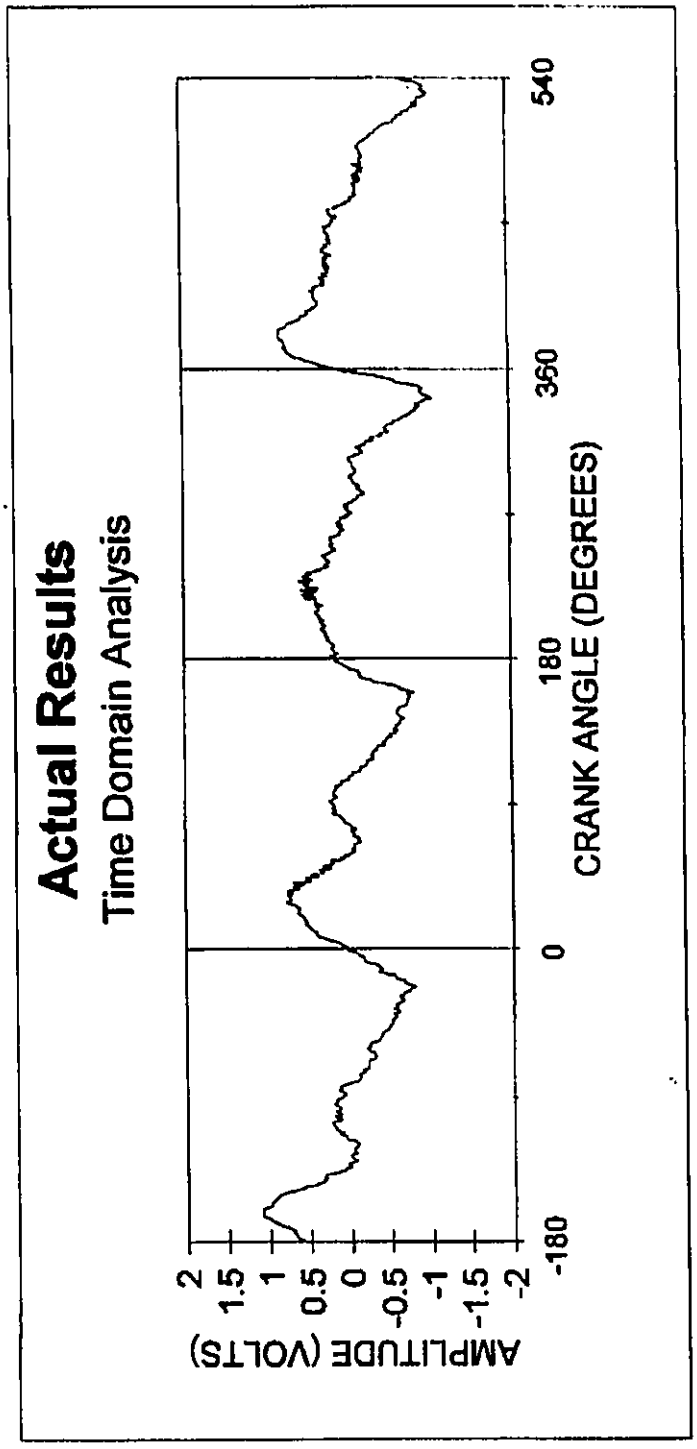

Figure 5.5: Time Domain Analysis for Actual Engine Signal

The experimental amplitude versus time output as measured by the LabView analysis program is illustrated in Figure 5.6. The general shape of the experimental time wave follows relatively close to that of the theoretical and actual time waves. The apexes that occur in the vicinity of the crank angles of 0 and 180 degrees appear to be somewhat premature. Alternatively, in the locality of -180 and 360 degrees, the peaks correspond closely to that of the other two time traces. The experimental plot also reveals sub-peaks proceeding the major summits which is counter to the other plots. It is suspected that these are the result of non-lineararities in the performance of the speakers used to produce the simulated pressure pulses at the manifold runner openings. Despite this, the misplacement of these sub-peaks does not alter the overall pattern similarities between this time analysis compared to the theoretical and actual plots. Although not evident in Figure 5.6, the period for this plot is 0.05 seconds which corresponds exactly to that of the theoretical time wave. Further, the displayed amplitudes at any given crank angle and relative maximum to minimum amplitudes correlate extremely well between all three of the time plots. As a result, even though each of the three plots display unique properties, they do all posses the same general qualitative characteristics which would allude that they each represent the same source, being the pressure wave at the throttle body outlet.

In addition to the above qualitative assessment, a quantitative evaluation comparing the time domain plots for the experimental model and actual neon engine was pursued using the statistical parameters discussed in section 4.2.2. The results of this evaluation are presented in Tables 1, 2 and 3.

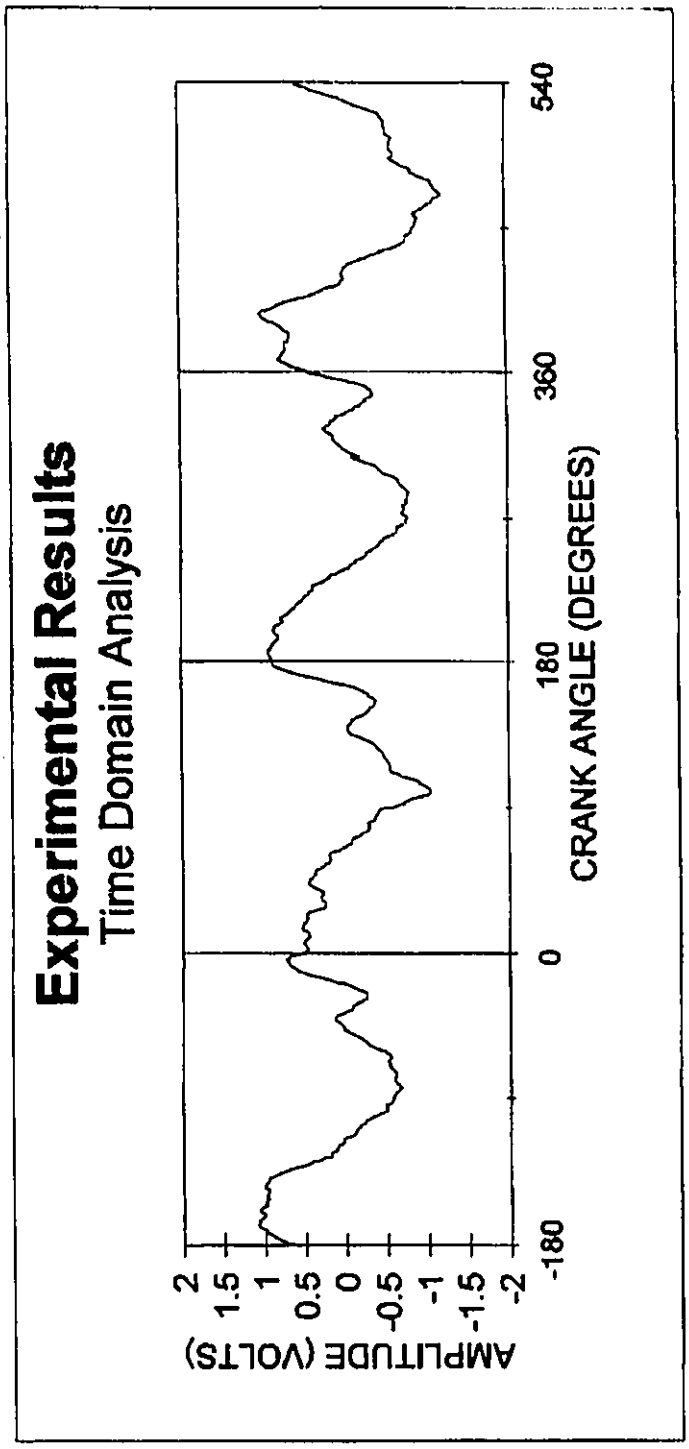

Figure 5.6: Time Domain Analysis for Experimental Signal

Table 1: Mean and Standard Deviation for Modelled and Actual Manifolds

Statistical Evaluation	Data Source	
	Simulation Model	Actual Engine
Mean	-0.02	0.01
Standard Deviation	0.58	0.45

Table 2: Correlation Matrix

	Simulation Model	Actual Engine
Simulation Model	1	-
Actual Engine	0.6	1

Table 3: Covariance Matrix

	Simulation Model	Actual Engine
Simulation Model	0.34	-
Actual Engine	0.16	0.21

The calculated mean values for the two curves remain fairly constant at zero volts indicating that both signals have the same central tendency as would be predicted for two similar data plots.

Similarly, both the experimental and the actual engine outputs have calculated standard deviations of 0.58 and 0.45 respectively. Therefore, not only do the two curves group about the same central value, but they do so with approximately the same measure of dispersion.

Perhaps the most convincing affinity between the two sets of data lie within the correlation and covariance analysis. The correlation coefficient between the two curves is 0.6 indicating a good correlation between the two plots. The covariance analysis resulted in a value of 0.16 indicating that the two curves trend in a similar manner. Given the great differences in the sources of the data for the two plots, the statistical analysis provided encouraging results. These quantitative observations serve only to reinforce the qualitative conclusions discussed earlier in justifying the high degree of similarity between the curves from the experimental model and actual neon engine.

5.2.2 **Results of Frequency Domain**

The frequency analysis for the theoretical output as described by the Ricardo Wave model is depicted in Figure 5.7. The results show that the output produced a fundamental frequency of 80 Hz followed by a second and third harmonic frequency of 160 and 240 Hz respectively. These results follow the expectations for a four cylinder engine operating at 2400 RPM. That is, a four cycle engine at 2400 RPM, or 40

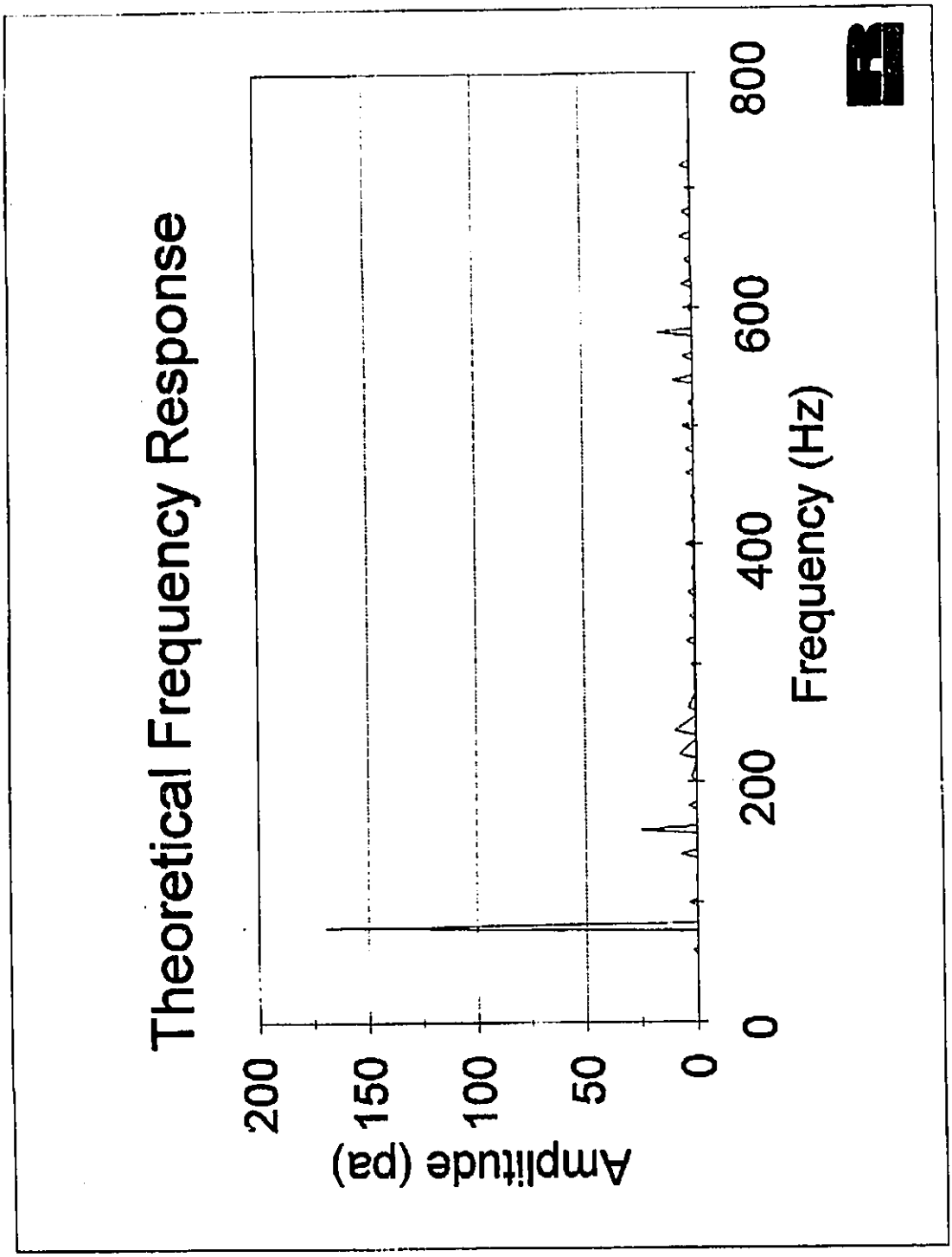

Figure 5.7: Theoretical Frequency Response from Ricardo Wave

revolution per second, would produce a fundamental frequency of 20 Hz for every combustion cycle. This multiplied by four, one for each cylinder, results in a fundamental frequency of 80 Hz. Given this reasoning, it is justified to accept the validity of the frequency analysis produced by the theoretical Ricardo Wave model.

The frequency response for the actual Neon engine is given in Figure 5.8. The first fundamental frequency is shown to be 74 Hz with 148 Hz and 222 Hz shown as the second and third harmonics respectively. This differs somewhat from the theoretical values but is not at all unexpected. As stated earlier, this is due to the fact that it was difficult for the dynamometer to maintain a constant speed of 2400 RPM with no ignition on the engine. It is estimated that the dynamometer was rotating the engine at approximately 2225 RPM thus resulting in the lower fundamental frequency. Despite these differences, the overall similarities between the actual engine results and the theoretical results proved that the effort was certainly worth while and that any short comings were due to the operation of the dynamometer equipment and not the analysis technique.

Figure 5.9 illustrates the LabView output for the frequency response for the simulation experiment. The results show that the output produced a fundamental frequency of 82 Hz followed by a second and third harmonic frequency of 160 and 240 Hz respectively. These results are very similar to the theoretical results indicating that the simulation model produced a frequency response that correlates closely to what it was predicted to. Only the first fundamental frequency differed from the theoretical outcome by a diminutive 2 Hz. The next two harmonics were identical to the theoretical

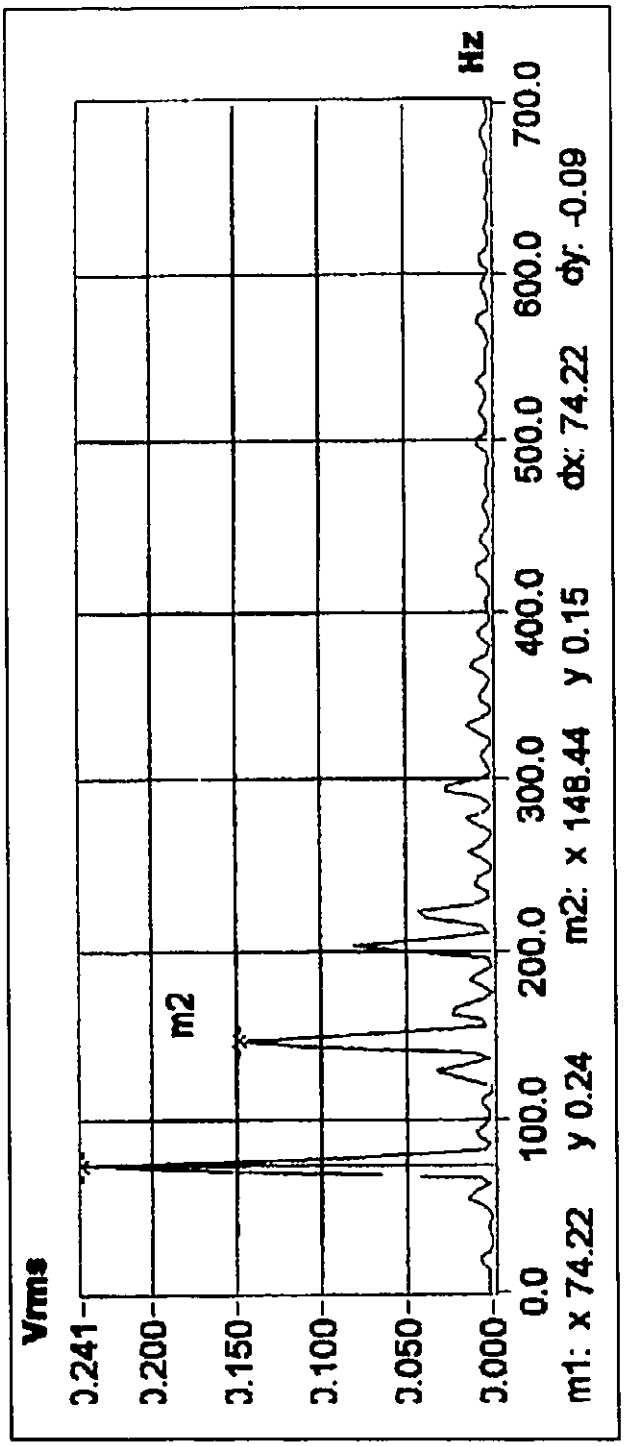

Figure 5.8: Frequency Response for Actual Neon Engine

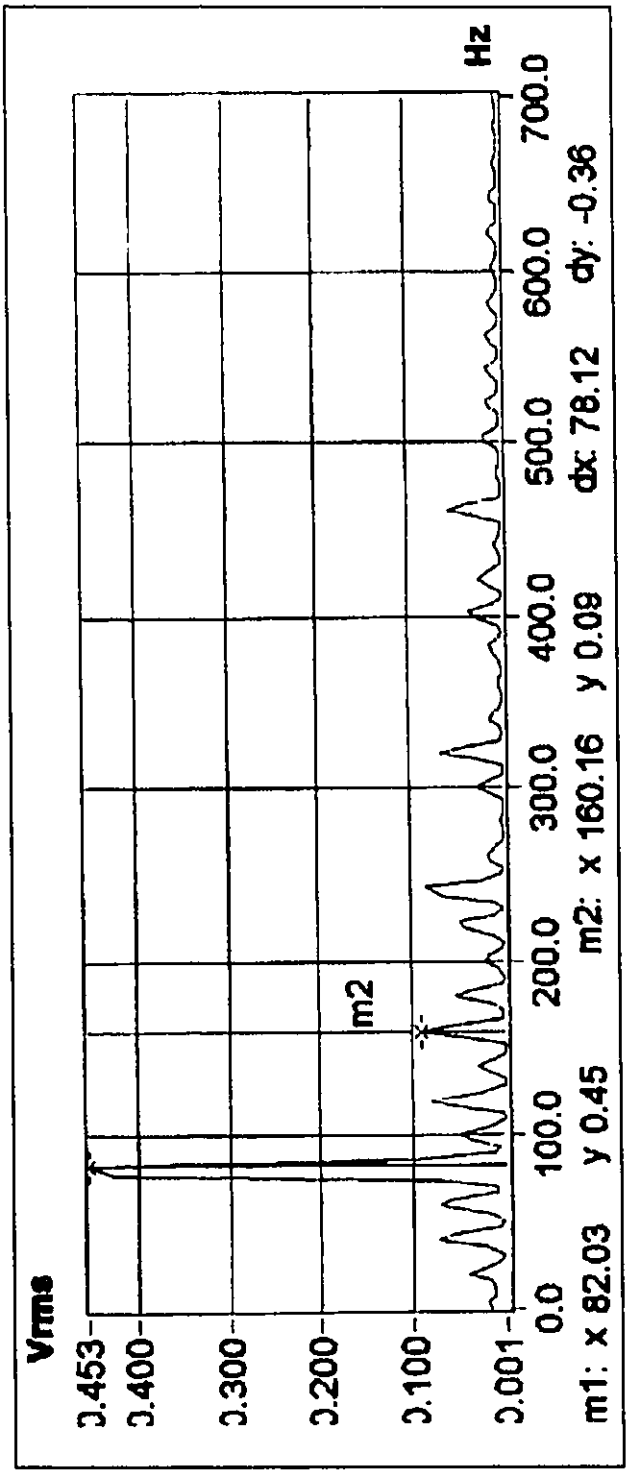

Figure 5.9: Frequency Response for Simulation Model

results. The reason for any differences between the experimental and actual engine results were again due to the dynamometer speed and not to any short comings associated with the experimental model.

VI. CONCLUSIONS AND RECOMMENDATION

6.1 Conclusions

The following is a list of conclusions that have been reached after studying the results of the data analysis.

1) Given the theoretical input signal at the interface between the intake manifold runner and engine head, it is possible to reproduce this signal. This allows for the simulation of the pressure pulses in the manifold runner caused by the opening and closing of the intake valves.
2) Analysis of the time domain signal for the actual Neon engine compared favourably to the theoretical time domain signal. This validates the use of either source as a reference for comparing the experimental results. Care must, however, be taken to ensure that the recorded period for the actual engine is accurate. That is, the dynamometer operating the engine must be turning at the correct speed.
3) The overall shape of the experimental time domain signal compared favourably to both the theoretical and actual engine results. The statistical parameters determined for the experimental and actual time domain signals also compared favourably to each other. It is suspected that any differences are the result of non-linearities in the low frequency operation of the speakers. The period of the experimental wave was identical to the theoretical time wave. This

reinforces the validity of the results associated with the experimental model and highlights the potential short comings with the actual measurements where precise period values are important.

4) The frequency distribution of all three sources were very similar. This reinforces the validity of the experimental simulation. The frequency results for the actual engine tests were the furthest away from the predicted results. This was again due to the inaccuracies in the dynamometer operation and not in the analysis procedure.

6.2 Recommendations

The creation and testing of the intake manifold simulation model has demonstrated great promise as a potential tool for simulating various operating parameters of the induction manifold. There are, however, some areas where additional efforts can be made to improve and verify this work.

1) The simulation experiment should be modified to allow the simulation at different engine RPMs. This would require the use of a faster computer among other things.
2) This simulation technique should be applied to other makes and configurations of intake manifolds. This would include expanding the equipment to accommodate six and eight cylinder engines.
3) It is recommended that the speakers used be replaced with others that are better able to reproduce signals in the lower frequency range.

4) Better control of the dynamometer used to drive the Neon automobile would result in more accurate measurements of the actual engine. It is thought that a dynamometer coupled directly to the engine as opposed to driving the automobile tires would aid in this effort.

REFERENCES

(1) Bruel & Kjaer, Electronic Instruments Master Catalogue, pp. 7.22-7.24, Bruel & Kjaer, Denmark, (1989).

(2) Daly, P.D., personal communication, (August, 1995).

(3) Fletcher, S., personal communication, (October, 1995).

(4) Lau, H.K., Statistical Assessment of Vibration Data in Drilling, M.A.Sc. Thesis, University of Windsor, Windsor, Ontario, (1987).

(5) Kraft, W.W., Sattler, E., Abboud, I., Noise Attenuation for Polyamide Intake Manifold, SAE Paper 950232, (1995).

(6) Miller, H.W., Piston Slap detection in Combustion Engines Using Unique Signal Analysis Techniques, M.A.Sc. Thesis, University of Windsor, Windsor, Ontario, (1989).

(7) Miller, I., Freund, J.E., Probability and Statistics for Engineers, 3rd Ed., Prentice-Hall Inc., Englewood Cliffs, NJ, (1985).

(8) National Instruments, Analysis VI Reference Manual, National Instruments, Austin, Texas, USA, (1994).

(9) National Instruments, Data Acquisition VI Reference Manual for Windows, National Instruments, Austin, Texas, USA, (1994).

(10) National Instruments, Instrumentation Reference and Catalogue, pp. 3.52-3.58, National Instruments, Austin, Texas, USA, (1994).

(11) National Instruments, Instrumentation Reference and Catalogue, pp. 3.47-3.53 National Instruments, Austin, Texas, USA, (1995).

(12) National Instruments, Instrupedia- Your Interactive Encyclopedia for Instrumentation, Vol. 1 No. 1, National Instruments, Austin, Texas, USA, (1995).

(13) Nelson, P., Transportation Noise Reference Book, Butterworth & Co., Cambridge, Great Britain, (1987).

(14) Nishio, Y. and Kuroda, O., New Approach to Low Noise Air Intake System Development, SAE Paper 911042, (1991).

(15) Novell PerfectOffice, Quattro Pro User's Guide, Wordperfect, Novell Applications Group, Orem, Utah, USA, (1994).

(16) Parsons, J.W., Reduction of Exhaust and Air Induction System Noise by a Predictive Method, SAE Paper 931338, (1993).

(17) Payri, F., Desantes, J.M., Salavert, J.M., Theoretical Validation of the Three Microphone Experimental Procedure, Universidad Politecnica de Valencia, Spain, (1990).

(18) Peat, K.S., Callow, G.D. and Bannister, P.A., Improving the Acoustic Performance of an Intake System, IMechE Paper C420/021, (1990).

(19) Randall, R.B., Frequency Analysis, 3rd Ed., Bruel & Kjaer, Denmark, (1987).

(20) Rejskind, G., The World of High Fidelity, Broadcast Canada, Longueuil, Quebec, (1994).

(21) Schellino, G., Vipiana, C., Guisset, P. and Sarti, S., Study of a Structural Acoustic Interaction in an Air Intake System for Commercial Vehicle,

APPENDIX A

Data Acquisition Equipment Specifications [12]

DATA ACQUISITION PRODUCTS

AT-AO-6, AT-AO-10

Analog Output Boards for the IBM PC AT

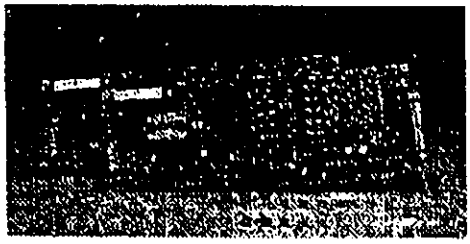

Features

* AT-AO-6 has 6 high-speed multiplying DACs
* AT-AO-10 has 10 high-speed multiplying DACs
* 12-bit resolution
* Unipolar or bipolar outputs available from each converter
* Voltage outputs from each converter
* 4 to 20 mA current sink to ground from each converter
* Onboard reference of 10 V
* 8-bit digital I/O (configurable in 4-bit ports)
* External bipolar reference input for each dual channel pair
* Double-buffered D/A latches with simultaneous update capability
* External update and interrupt request signals
* DMA and interrupt capability for waveform generation applications
* 1-Kword FIFO for high continuous throughput
* Counter/timer for periodic interrupt or dma request
* Software calibration
* Programmed with LabVIEW, LabWindows/CVI, and LabWindows

Overview

The National Instruments AT-AO-6 and AT-AO-10 are high-performance, 12-bit analog output boards for the IBM AT and compatibles. They have either 6 or 10 identical DAC channels, each of which has voltage output and can sink 4 to 20 mA current when connected to an external source. Because these boards are identical except for output channel count, they will be described in common and referred to as the AT-AO-6/10. The voltage output of each channel is either bipolar or unipolar and is derived from the onboard reference or an external reference. An 8-bit DIO port provides additional control capability. Software-controlled calibration eliminates removing the PC cover and manually adjusting trimpots.

AT-AO-6, AT-AO-10

Specifications

Typical for 25 degrees C unless otherwise noted

Analog Output

Output Characteristics

Number of channels	
AT-AO-6	6 voltage or current
AT-AO-10	10 voltage or current
Resolution	12 bits, 1 in 4,096
Maximum update rate	300 kS/s, system dependent
Type of DAC	Double-buffered, multiplying
FIFO buffer size	1,024 samples
Data transfers	DMA, interrupts, programmed I/O
DMA modes	Single transfer

Transfer Characteristics

Relative accuracy (INL)	+/- 0.5 LSB maximum
Absolute accuracy	+/- 0.01 % FSR typical, +/- 0.02% maximum
DNL	+/- 0.2 LSB typical, +/- 1.0 LSB maximum
Monotonicity	12 bits, guaranteed
Offset error	
After calibration	1 mV maximum
Before calibration	200 mV maximum
Gain error (relative to internal reference)	
After calibration	+/- 0.01% of reading maximum
Before calibration	+/- 0.5% of reading maximum
Gain error (relative to external reference)	+/- 0.1% of reading maximum, not adjustable

Voltage Output

Ranges	+/- 10 V, +/- Vref or 0 to 10 V, 0 to
Vref jumper selectable	
Output coupling	DC
Output impedance	0.1 Omega maximum
Current drive	+/- 5mA maximum
Load impedance	500 pf maximum
Protection	short circuit to ground
Power on state	0 V bipolar, 5 V unipolar range
External reference input	
Range	+/- 10 V
Overvoltage protection	+/- 25 V powered on, +/- 25 V powered off
Input impedance	10 kOmega
Bandwidth (-3 dB)	1 MHz

Current Output

Range	4 to 20 mA
Type	Sink to ground, requires external excitation source
Output impedance	1 GOmega minimum
Excitation voltage range	+7 to +40 V
Absolute accuracy	+/- 0.1% FSR
Slew rate	7.5 mA/ us
Protection	Short circuit to ground and open circuit

Power-on state	4 mA bipolar, 12 mA unipolar
Dynamic Characteristics	
Settling time to +/- 0.01% FSR	
[Image]	
Slew rate	10 V/ us minimum
Stability	
Offset temperature coefficient	+/- 50 uV/ degreesC
Gain temperature coefficient	
Internal reference	+/- 10 ppm/ degreesC
External reference	+/- 5 ppm/ degreesC
Digital I/O	
Number of channels	8 I/O
Compatibility	TTL
Digital logic levels	
[Image]	
Power-on state	Configured as inputs
Data transfers	Programmed I/O
RTSI	
Trigger	lines 7
Bus Interface	Slave
Power Requirement	
AT-AO-6	
+5 VDC (+/- 5%)	0.6A
+12 VDC (+/- 5%)	60 mA + load
-12 VDC (+/- 5%)	60 mA + load
AT-AO-10	
+5 VDC (+/- 5%)	1.6 A
Physical	
Dimensions	34.0 by 11.4 cm (13.3 by 4.5 in.)
I/O connector	50-pin male
Environment	
Operating temperature	0 degrees to 70 degrees C
Storage temperature	-55 degrees to 150 degrees C
Relative humidity	5% to 90% noncondensing

Data Acquisition Products

AT-A2150

Dynamic Signal Acquisition Board for the PC AT

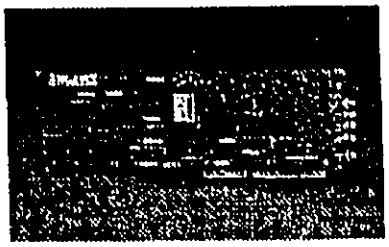

Features

* Two models with sampling rates tailored to application areas
- AT-A2150C for general audio band measurements and industry-standard analysis sampling rates
- AT-A2150S for speech and voice band measurements
* High-accuracy analog inputs
- 4 analog input channels with simultaneous sampling
- 16-bit resolution delta-sigmamodulating ADCs
- Linear-phase antialiasing filters attenuate 90 dB in 1/6 octave
- 93 dB SNR for low-noise signal acquisition
- -95 dB THD for high accuracy
- +/-2.828 V input range (2 Vrms)
- Software-programmable AC/DC coupling
* External trigger input can control data acquisition
- Pretrigger, posttrigger, and delay trigger mode
- Level-and-slope detection circuitry to trigger on programmed level and slope on any analog input channel
- Digital trigger control from I/O connector, RTSI bus, or software
* RTSI bus interface
- Multiple-board sampling and/or trigger synchronization
* Programmed with LabVIEW, LabWindows/CVI, and LabWindows

Overview

The AT-A2150 is a high-accuracy, dynamic signal acquisition plug-in board for scientific class measurements with IBM PC AT and compatibles. The AT-A2150C digitizes signals over a bandwidth from DC to20kHz, and the AT-A2150S digitizes signals over a bandwidth of DC to 10 kHz. The boards have four 16bit analog input channels with antialiasing filters and 64-times oversampling delta-sigma modulating ADCs. The antialiasing filters on the input ensure that signals are acquired with extremely high fidelity. A 93 dB SNR, -95 dB THD, and +/-0.025 dB amplitude flatness make it possible to acquire signals with extremely high accuracy and low noise.

The interface to the PC ATI/O channel has FIFO buffers to prevent data loss if DMA or interrupt service latency is long. Flexible pretrigger, posttrigger, and delay trigger modes make it possible to acquire signals when desired.

The AT-A2150 has the National Instruments RTSI bus to synchronize the sampling and/or triggering of multiple AT-A2150 boards. RTSI is a dedicated system timing and communications bus, implemented with a ribbon cable and connected directly between AT-Series boards.

DATA ACQUISITION PRODUCTS

AT-A2150

Specifications

Typical for 25 degrees C unless otherwise noted. Refer to the Data Acquisition Overview for typical frequency response plots.

Analog Input

Input Characteristics

Number of channels	4 single-ended, simultaneously sampled
Type of ADC	Delta-sigma
Resolution	16 bits, 1 in 65,536

Sampling Rates

AT-A2150S	2.0, 2.5, 3.0, 4.0, 5.0, 6.0, 8.0, 10.0, 12.0, 16.0, 20.0, and 24.0 kS/s
AT-A2150C	4.0, 5.5125, 6.0, 6.4, 8.0, 11.025, 12.0, 12.8, 16.0, 22.05, 24.0, 25.6, 32.0, 44.1, 48.0, and 51.2 kS/s
Input signal range	+/- 2.828 V (2 Vrms)
Input coupling	AC or DC, software selectable
Overvoltage protection	+/- 20 V powered on or off
Inputs protected	ACH0, ACH1, ACH2, ACH3
Data transfers	DMA, interrupts, programmed I/O

Transfer Characteristics

Offset error after calibration	+/- 5 LSB typical, +/- 15 LSB maximum
Gain adjustment range	+/- 3.5% (+/- 0.3 dB)

Amplifier Characteristics

Input impedance	
Normal powered on	460 kOhms in parallel with 75 pF

Dynamic Characteristics

Bandwidth (-3 dB)	DC to 0.45 times sampling rate, DC coupled 8.8 Hz to 0.45 times sampling rate, AC couple
System noise (including quantization error)	0.5 LSBrms
Dynamic range	93 dB
Signal-to-THD plus noise	90 dB for 0 dB input, DC to 22 kHz
THD	-95 dB for 0 dB input, DC to 22 kHz

Amplitude Flatness

AT-A2150C	+/- 0.01 dB typical, +/- 0.025 dB maximum, DC to 20 kHz (48 kS/s sampling rate)
AT-A2150S	+/- 0.01 dB typical, +/- 0.025 dB maximum, DC to 4 kHz +/- 0.05 dB maximum, DC to10 kHz (24 kS/s sampling rate)
Phase linearity	+/- 0.5 degrees, DC to 20 kHz
Interchannel phase	+/- 1 degrees, DC to 20 kHz
IMD	

SMPTE	(60 Hz, 7 kHz) -85 dB
DIN	(250 Hz, 8 kHz) -85 dB
CCIF	(14 kHz, 15 kHz) -95 dB
Crosstalk	-90 dB, DC to 22 kHz

Filters

Type	Analog and digital antialiasing
Passband ripple	+/- 0.01 dB pk-pk, DC to 20 kHz
Stopband attenuation	86 dB
Attenuation rate	90 dB in 1/6 octave
Signal delay	35.6 sample periods

Triggers

Digital Trigger	
Compatibility	TTL
Response	Programmable for rising or falling edge
Pulse width	50 ns

RTSI

Trigger lines	1
DMA channels	2
Serial links	2 full duplex
Serial transfer rate	1.6384 Mb/s

Power Requirement

+5 VDC	1.5 A

Physical

Dimensions	33.6 by 11.4 cm (13.25 by 4.5 in.)
I/O connector	RCA-type phono jacks

Environment

Component operating temperature	0 degrees to 70 degrees C
Component storage temperature	-55 degrees to 150 degrees C
Relative humidity	5% to 90% noncondensing

APPENDIX B

Input Data From Ricardo Wave Model

Cylinder Pressure Data

Crank Angle For Cyl. 3	Cylinder Number			
	Cyl.3	Cyl. 4	Cyl. 2	Cyl. 1
-180	0.796164	0.997826	0.985245	0.98582
-177.517241	0.802315	1.0019	0.984975	0.985519
-175.034483	0.808594	1.00659	0.984743	0.985485
-172.551724	0.983931	0.687885	0.985008	0.986212
-170.068966	0.984082	0.688027	0.985388	0.9865
-167.586207	0.983836	0.688386	0.985186	0.986282
-165.103448	0.984069	0.68895	0.985253	0.98624
-162.62069	0.984773	0.689719	0.985745	0.986575
-160.137931	0.984971	0.690692	0.986038	0.986553
-157.655172	0.984771	0.691869	0.985651	0.986133
-155.172414	0.985003	0.693253	0.985244	0.985976
-152.689655	0.985196	0.694851	0.98537	0.986274
-150.206897	0.984468	0.696667	0.98516	0.986279
-147.724138	0.98355	0.6987	0.984752	0.986002
-145.241379	0.983674	0.700908	0.98482	0.986156
-142.758621	0.984083	0.703352	0.98545	0.986389
-140.275862	0.983915	0.706022	0.985735	0.986195
-137.793103	0.984039	0.708866	0.985405	0.986866
-135.310345	0.984794	0.71188	0.985414	0.98608
-132.827586	0.985043	0.715084	0.985543	0.986525
-130.344828	0.984389	0.718461	0.98542	0.986631
-127.862069	0.984061	0.722004	0.985126	0.986718
-125.37931	0.984372	0.725729	0.985388	0.986915
-122.896552	0.984448	0.729643	0.985972	0.986906
-120.413793	0.984238	0.733742	0.986025	0.986419
-117.931034	0.984357	0.738025	0.985771	0.98591
-115.448276	0.984764	0.742499	0.985523	0.985827
-112.965517	0.984712	0.747157	0.985426	0.98596
-110.482759	0.984208	0.751988	0.985046	0.986156
-108	0.983929	0.756981	0.984746	0.986398
-105.517241	0.984113	0.762134	0.985005	0.986954
-103.034483	0.984353	0.767439	0.985505	0.987688
-100.551724	0.984322	0.772895	0.985852	0.988553
-98.0689655	0.984487	0.778501	0.985828	0.989779
-95.5862069	0.984962	0.784252	0.985962	0.991692
-93.1034483	0.985245	0.790142	0.986003	0.994443
-90.6206896	0.984975	0.796164	0.98582	0.997826
-88.137931	0.984743	0.802315	0.985519	1.0019
-85.6551724	0.984885	0.808594	0.985485	1.00659
-83.1724138	0.984885	0.815	0.985662	1.01179
-80.6896552	0.984525	0.821537	0.985618	1.01714
-78.2068965	0.984273	0.828225	0.985527	1.02197
-75.7241379	0.984401	0.835099	0.985455	1.02608
-73.2413793	0.984434	0.84219	0.98555	1.02781
-70.7586207	0.984342	0.849504	0.98561	1.02583
-68.2758621	0.984456	0.857019	0.985531	1.01898

-65.7931034	0.984838	0.864699	0.985593	1.00778
-63.3103448	0.985011	0.872503	0.985722	0.99287
-60.8275862	0.985192	0.880391	0.985818	0.974652
-58.3448276	0.985025	0.888315	0.985868	0.95527
-55.862069	0.984947	0.896236	0.985904	0.937054
-53.3793103	0.984788	0.904114	0.985864	0.919738
-50.8965517	0.984788	0.911896	0.985974	0.903839
-48.4137931	0.98483	0.919516	0.986055	0.890969
-45.9310345	0.984846	0.926909	0.986056	0.880235
-43.4482758	0.98506	0.934016	0.985784	0.869681
-40.9655172	0.98506	0.940777	0.985611	0.859538
-38.4827586	0.984968	0.94714	0.985486	0.849383
-36	0.984517	0.953063	0.985359	0.83822
-33.5172414	0.984372	0.958525	0.985256	0.826118
-31.0344827	0.984465	0.963519	0.985473	0.81381
-28.5517241	0.984719	0.968075	0.986013	0.801608
-26.0689655	0.985025	0.972288	0.986343	0.789974
-23.5862069	0.985317	0.97623	0.986381	0.77963
-21.1034483	0.985777	0.979805	0.986248	0.770777
-18.6206896	0.985695	0.982627	0.986222	0.76335
-16.137931	0.985266	0.984504	0.985964	0.756818
-13.6551724	0.984771	0.985476	0.985584	0.751011
-11.1724138	0.984712	0.985775	0.985528	0.745465
-8.68965515	0.984765	0.985549	0.985896	0.73995
-6.20689653	0.984577	0.984797	0.98619	0.734394
-3.72413791	0.984821	0.984077	0.98599	0.728976
-1.24137929	0.985224	0.983705	0.985885	0.723835
1.241379333	0.98597	0.983296	0.985957	0.719128
3.724137954	0.984967	0.982926	0.985829	0.714885
6.206896575	0.984881	0.985631	0.985512	0.711084
8.689655196	0.985273	0.985193	0.985694	0.707658
11.17241382	0.985243	0.984952	0.986368	0.704526
13.65517244	0.985128	0.984128	0.986571	0.701641
16.13793106	0.985326	0.98334	0.986406	0.698992
18.62068968	0.985702	0.983357	0.986446	0.696597
21.1034483	0.985471	0.983289	0.986509	0.694478
23.58620692	0.984951	0.982655	0.986066	0.692652
26.06896554	0.985077	0.982358	0.985552	0.691128
28.55172416	0.985193	0.98279	0.985741	0.689907
31.03448278	0.98496	0.983046	0.986019	0.688982
33.51724141	0.984711	0.982911	0.985895	0.688346
36.00000003	0.985008	0.98326	0.985849	0.687985
38.48275865	0.985388	0.983931	0.986212	0.687885
40.96551727	0.985186	0.984082	0.9865	0.688027
43.44827589	0.985253	0.983836	0.986282	0.688386
45.93103451	0.985745	0.984069	0.98624	0.68895
48.41379313	0.986038	0.984773	0.986575	0.689719
50.89655175	0.985651	0.984971	0.986553	0.690692
53.37931037	0.985244	0.984771	0.986133	0.691869
55.86206899	0.98537	0.985003	0.985976	0.693253

58.34482762	0.98516	0.985196	0.986274	0.694631
60.82758624	0.984752	0.984468	0.986279	0.696667
63.31034486	0.98482	0.98355	0.986002	0.6987
65.79310348	0.98545	0.983674	0.986156	0.700908
68.2758621	0.985735	0.984083	0.986389	0.703352
70.75862072	0.985405	0.983915	0.986195	0.706022
73.24137934	0.985414	0.984039	0.985866	0.708866
75.22413796	0.985543	0.984794	0.98608	0.71188
78.70689658	0.98542	0.985043	0.986525	0.715084
81.1896552	0.985126	0.984389	0.986631	0.718461
83.67241383	0.985388	0.984061	0.986718	0.722004
86.15517245	0.985972	0.984372	0.986915	0.725729
88.63793107	0.986025	0.984448	0.986906	0.729643
91.12068969	0.985771	0.984238	0.986419	0.733742
93.60344831	0.985523	0.984357	0.98591	0.738025
96.08620693	0.985426	0.984764	0.985827	0.742499
98.56896555	0.985046	0.984712	0.98596	0.747157
101.0517242	0.984746	0.984208	0.986156	0.751988
103.5344828	0.985005	0.983929	0.986398	0.756981
106.0172414	0.985505	0.984113	0.986954	0.762134
108.5	0.985852	0.984353	0.987688	0.767439
110.9827587	0.985828	0.984322	0.988553	0.772895
113.4655173	0.985962	0.984487	0.989779	0.778501
115.9482759	0.986003	0.984962	0.991692	0.784252
118.4310345	0.98582	0.985245	0.994443	0.790142
120.9137931	0.985519	0.984975	0.997826	0.796164
123.3965518	0.985485	0.984743	1.0019	0.802315
125.8793104	0.985662	0.984885	1.00659	0.808594
128.362069	0.985618	0.984885	1.01179	0.815
130.8448276	0.985527	0.984525	1.01714	0.821537
133.8275862	0.985455	0.984273	1.02197	0.828225
136.2931449	0.98555	0.984401	1.02608	0.835099
138.7759035	0.98551	0.984434	1.02781	0.84219
141.2586621	0.985531	0.984342	1.02583	0.849504
143.7414207	0.985593	0.984456	1.01898	0.857019
146.2241794	0.985722	0.984838	1.00778	0.864699
148.706938	0.985818	0.985011	0.99287	0.872503
151.1896966	0.985868	0.985192	0.974652	0.880391
153.6724552	0.985904	0.985025	0.95527	0.888315
156.1552138	0.985864	0.984947	0.937054	0.896236
158.6379725	0.985974	0.984788	0.919738	0.904114
161.1207311	0.986055	0.984788	0.903839	0.911896
163.6034897	0.986056	0.98483	0.890969	0.919516
166.0862483	0.985784	0.984846	0.880235	0.926909
168.5690069	0.985611	0.98506	0.869681	0.934016
171.0517656	0.985486	0.98506	0.859538	0.940777
173.5345242	0.985359	0.984968	0.849383	0.94714
176.0172828	0.985256	0.984517	0.83822	0.953063
178.5000414	0.985473	0.984372	0.826118	0.958525
180.9828	0.986013	0.984465	0.81381	0.963519

183.4655587	0.986343	0.984719	0.801606	0.968075
185.9483173	0.986381	0.985025	0.789974	0.972288
188.4310759	0.986248	0.985317	0.77963	0.97623
190.9138345	0.986222	0.985777	0.770777	0.979805
193.3965931	0.985964	0.985695	0.76335	0.982627
195.8793518	0.985584	0.985266	0.756818	0.984504
198.3621104	0.985528	0.984771	0.751011	0.985476
200.844869	0.985896	0.984712	0.745465	0.985775
203.3276276	0.98619	0.984765	0.73995	0.985549
205.8103863	0.98599	0.984577	0.734394	0.984797
208.2931449	0.985886	0.984821	0.728976	0.984077
210.7759035	0.985957	0.985224	0.723835	0.983705
213.2586621	0.985829	0.98537	0.719128	0.983296
215.7414207	0.985512	0.984967	0.714885	0.982926
218.2241794	0.985694	0.984881	0.711084	0.985631
220.706938	0.986368	0.985273	0.707658	0.985193
223.1896966	0.986571	0.985243	0.704626	0.984952
225.6724552	0.986406	0.985128	0.701641	0.984128
228.1552138	0.986446	0.985326	0.698992	0.98334
230.6379725	0.986509	0.985702	0.696597	0.983357
233.1207311	0.986066	0.985471	0.694478	0.983289
235.6034897	0.985552	0.984951	0.692652	0.982655
238.0862483	0.985741	0.985077	0.691128	0.982358
240.5690069	0.986019	0.985193	0.689907	0.98279
243.0517656	0.985895	0.98496	0.688982	0.983046
245.5345242	0.985849	0.984711	0.688346	0.982911
248.0172828	0.986212	0.985008	0.687985	0.98326
250.5000414	0.9865	0.985388	0.687885	0.983931
252.9828001	0.986282	0.985186	0.688027	0.984082
255.4655587	0.98624	0.985253	0.688386	0.983836
257.9483173	0.986575	0.985745	0.68895	0.984069
260.4310759	0.986553	0.986038	0.689719	0.984773
262.9138345	0.986133	0.985651	0.690692	0.984971
265.3965932	0.985976	0.985244	0.691869	0.984771
267.8793518	0.986274	0.98537	0.693253	0.985003
270.3621104	0.986279	0.98516	0.694851	0.985196
272.844869	0.986002	0.984752	0.696667	0.984468
275.3276276	0.986156	0.98482	0.6987	0.98355
277.8103863	0.986389	0.98545	0.700908	0.983674
280.2931449	0.986195	0.985735	0.703352	0.984083
282.7759035	0.985866	0.985405	0.706022	0.983915
285.2586621	0.98608	0.985414	0.708866	0.984039
287.7414207	0.986525	0.985543	0.71188	0.984794
290.2241794	0.986631	0.98542	0.715084	0.985043
292.706938	0.986718	0.985126	0.718461	0.984389
295.1896966	0.986915	0.985388	0.722004	0.984061
297.6724552	0.986906	0.985972	0.725729	0.984372
300.1552139	0.986419	0.986025	0.729643	0.984448
302.6379725	0.98591	0.985771	0.733742	0.984238
305.1207311	0.985827	0.985523	0.738025	0.984357

307.6034897	0.98596	0.985426	0.742499	0.964764
310.0862483	0.986156	0.985046	0.747157	0.984712
312.569007	0.986398	0.984746	0.751988	0.984208
316.0517656	0.986954	0.985005	0.756981	0.983929
317.5345242	0.987686	0.986505	0.762134	0.984113
320.0172828	0.988553	0.985852	0.767439	0.984353
322.5000414	0.989779	0.985828	0.772895	0.984322
325.4828001	0.991692	0.985962	0.778501	0.984487
327.9655587	0.994443	0.986003	0.784252	0.984962
330.4483173	0.997826	0.98582	0.790142	0.985245
332.9310759	1.0019	0.985519	0.796164	0.984975
335.4138345	1.00659	0.985485	0.802315	0.984743
337.8965932	1.01178	0.985662	0.808594	0.984885
340.3793518	1.01714	0.985618	0.815	0.984885
342.8621104	1.02197	0.985527	0.821537	0.984525
345.344869	1.02608	0.985455	0.828225	0.984273
347.8276277	1.02781	0.98555	0.835099	0.984401
350.3103863	1.02583	0.98551	0.84219	0.984434
352.7931449	1.01898	0.985531	0.849504	0.984342
355.2759035	1.00778	0.985593	0.857019	0.984456
357.7586621	0.99287	0.985722	0.864699	0.984838
360.2414208	0.974652	0.985818	0.872503	0.985011
362.7241794	0.95527	0.985868	0.880391	0.985192
365.206938	0.937054	0.985904	0.888315	0.985025
367.6896966	0.919738	0.985864	0.896236	0.984947
370.1724552	0.903839	0.985974	0.904114	0.984788
372.6552139	0.890969	0.986055	0.911896	0.984788
375.1379725	0.880235	0.986056	0.919516	0.98483
377.6207311	0.869681	0.985784	0.926909	0.984846
380.1034897	0.859538	0.985611	0.934016	0.98506
382.5862483	0.849383	0.985486	0.940777	0.98506
385.569007	0.83822	0.985359	0.94714	0.984968
388.5517656	0.826118	0.985256	0.953063	0.984517
391.0345242	0.81381	0.985473	0.958525	0.984372
393.5172828	0.801608	0.986013	0.963519	0.984465
396.0000415	0.789974	0.986343	0.968075	0.984719
398.4828001	0.77963	0.986381	0.972288	0.985025
400.9655587	0.770777	0.986248	0.97623	0.985317
403.4483173	0.76335	0.986222	0.979805	0.985777
405.9310759	0.756818	0.985964	0.982627	0.985685
408.4138346	0.751011	0.985584	0.984504	0.985286
410.8965932	0.745465	0.985528	0.985476	0.984771
413.3793518	0.73995	0.985896	0.985775	0.984712
415.8621104	0.734394	0.98619	0.985549	0.984765
418.344869	0.728976	0.98599	0.984797	0.984577
420.8276277	0.723835	0.985885	0.984077	0.984821
423.3103863	0.719128	0.985957	0.983705	0.985224
425.7931449	0.714885	0.985829	0.983296	0.98537
428.2759035	0.711084	0.985512	0.982926	0.984967
430.7586621	0.707658	0.985694	0.985631	0.984881

433.2414208	0.704525	0.986368	0.985193	0.985273
435.7241794	0.701641	0.986571	0.984952	0.985243
438.206938	0.698992	0.986406	0.984128	0.985128
440.6896966	0.696597	0.986446	0.98334	0.985326
443.1724553	0.694478	0.986509	0.983357	0.985702
445.6552139	0.692652	0.986066	0.983289	0.985471
448.1379725	0.691128	0.985552	0.982655	0.984951
450.6207311	0.689907	0.985741	0.982358	0.985077
453.1034897	0.688982	0.986019	0.98279	0.985193
455.5862484	0.688346	0.985895	0.983046	0.98496
458.069007	0.687985	0.985849	0.982911	0.984711
460.5517656	0.687885	0.986212	0.98326	0.985008
463.0345242	0.688027	0.9865	0.983931	0.985388
465.5172828	0.688386	0.986282	0.984082	0.985186
468.0000415	0.68895	0.98624	0.983836	0.985253
470.4828001	0.689719	0.986575	0.984069	0.985745
472.9655587	0.690692	0.986553	0.984773	0.986038
475.4483173	0.691869	0.986133	0.984971	0.985651
477.9310759	0.693253	0.985976	0.984771	0.985244
480.4138346	0.694851	0.986274	0.985003	0.98537
482.8965932	0.696667	0.986279	0.985196	0.98516
485.3793518	0.6987	0.986002	0.984468	0.984752
487.8621104	0.700908	0.986156	0.98355	0.98482
490.344869	0.703352	0.986389	0.983674	0.98545
492.8276277	0.706022	0.986195	0.984083	0.985735
495.3103863	0.708866	0.985866	0.983915	0.985405
497.7931449	0.71188	0.98608	0.984039	0.985414
500.2759035	0.715084	0.986525	0.984794	0.985543
502.7586622	0.718461	0.986631	0.985043	0.98542
505.2414208	0.722004	0.986718	0.984389	0.985126
507.7241794	0.725729	0.986915	0.984061	0.985388
510.206938	0.729643	0.986906	0.984372	0.985972
512.6896966	0.733742	0.986419	0.984448	0.986025
515.1724553	0.738025	0.98591	0.984238	0.985771
517.6552139	0.742499	0.985827	0.984357	0.985523
520.1379725	0.747157	0.98596	0.984764	0.985426
522.6207311	0.751988	0.986156	0.984712	0.985046
525.1034897	0.756981	0.986398	0.984208	0.984746
527.5862484	0.762134	0.986954	0.983929	0.985005
530.069007	0.767439	0.987688	0.984113	0.985505
532.5517656	0.772895	0.988553	0.984353	0.985862
535.0345242	0.778501	0.989779	0.984322	0.985828
537.5172828	0.784252	0.991692	0.984487	0.985962
540.0000415	0.790142	0.994443	0.984982	0.986003

APPENDIX C

Description of LabView Subprograms

AO Config.vi

device (1)

device is the device number you assigned to the plug-in DAQ board during configuration. This parameter defaults to 1. For information about configuration, refer to Chapter 2, Getting Started with the Data Acquisition VIs.

taskID

taskID uniquely identifies the device, group, and I/O operation. Use this value as the taskID to refer to this group in subsequent VI calls.

error out

error out contains error information. If the error in cluster indicated an error, the error out cluster contains the same values as the corresponding elements of error in. If error in did not indicate an error, error out describes the error status produced by this VI.

channels (0)

channels is an array of strings that specifies the set of analog output channels for a group and task. You cannot list a channel more than once. The default input is channel 0.

buffer size
(1000 updates)

buffer size is the number of updates you want the buffer to hold. The default input is 1,000 updates. Remember, an update is defined as one data point for each channel in the channels array.

error in (no error)

error in describes error conditions occuring before this VI executes. If an error has already occurred, this VI does not perform any configuration and passes the error in to the error out cluster.

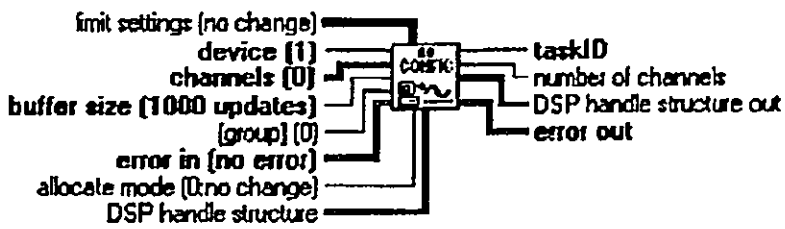

AO Config.vi

Most applications need only connect wires to the controls and indicators displayed in bold. Connections to other controls and indicators are useful only if specifically needed.

Configures an analog output operation for a specified set of channels.

AO Start.vi

taskID in

task ID in identifies the group and I/O operation.

taskID out

taskID out has the same value as taskID in.

error in (no error)

error in describes error conditions occurring before this VI executes. If an error has already occurred, this VI does not write the data to the buffer and passes the error in to the error out cluster.

update rate
(1000 updates/sec)

update rate is the number of updates to generate per second. The default input is 1000 updates/s, which means that each channel in the group is written to (updated) 1000 times per second.

error out

error out contains error information. If the error in cluster indicated an error, the error out cluster contains the same information. Otherwise, error out describes the error status of this VI.

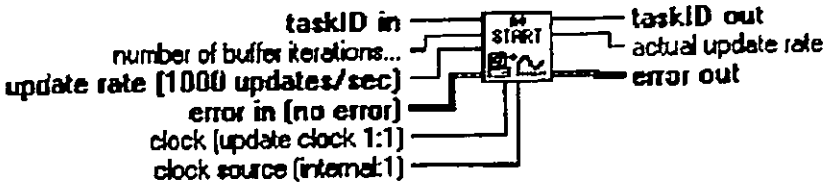

AO Start.vi

Most applications need only connect wires to the controls and indicators displayed in bold. Connections to other controls and indicators are useful only if specifically needed.

Starts a buffered analog output operation. AO Start sets the update rate and then starts the generation.

AO Write.vi

taskID in

taskID in identifies the group and I/O operation.

taskID out

taskID out has the same value as taskID in.

error in (no error)

error in describes error conditions occurring before this VI executes. If an error has already occurred, this VI does not write the data to the buffer and passes the error in to the error out cluster.

voltage data

voltage data is a 2D array that contains data to be written to the buffer in volts or milliamperes. If you have more than one channel in your group, you must arrange your data in columns. The bottom dimension selects which column and which channel.

error out

error out contains error information. If the error in cluster indicated an error, the error out cluster contains the same information. Otherwise, error out describes the error status of this VI.

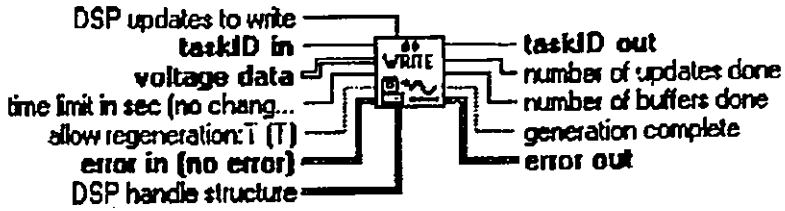

AO Write.vi

Most applications need only connect wires to the controls and indicators displayed in bold. Connections to other controls and indicators are useful only if specifically needed.

Writes data into the buffer for a buffered analog output operation.

Reading Data from Spreadsheet

number of rows (all:-1)

number of rows is the maximum number of rows or lines the VI reads. The default value is -1.

all rows

all rows is the data read from the file in the form of a 2D array of single-precision numbers.

file path (dialog if empty)

file path is the path name of the file. If file path is empty (default value) or is Not A Path, the VI displays a File dialog box from which you can select a file. Error 43 occurs if the user cancels the dialog.

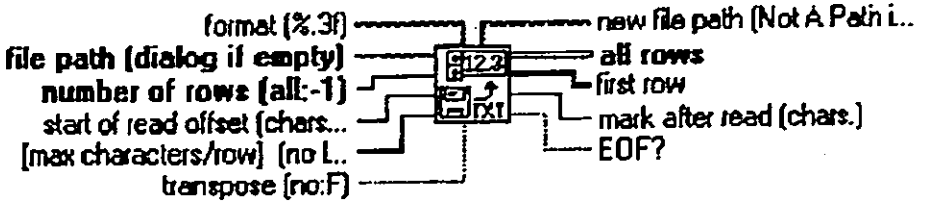

Read From Spreadsheet File.vi

Reads a specified number of lines or rows from a numeric text file beginning at a specified character offset and converts the data to a 2D single-precision array of numbers. You can optionally transpose the array. The VI opens the file beforehand and closes it afterwards.

VITA AUCTORIS

1968	Born in Toronto, Ontario on February 20.
1987	Received OSSGHD from Brampton Centennial Secondary School.
1991	Received Degree of Bachelor of Applied Science from the University of Windsor, Windsor, Ontario.
1993	Received Professional Engineer Licence from the Association of Professional Engineers of Ontario.
1996	Candidate for the Degree of Master of Applied Science at the University of Windsor, Windsor, Ontario.